doi:10.1093/brain/awq107 Brain 2010: 133; 2264–2280 | 2264

BRAIN
A JOURNAL OF NEUROLOGY

Neuroprotection in a rabbit model of intraventricular haemorrhage by cyclooxygenase-2, prostanoid receptor-1 or tumour necrosis factor-alpha inhibition

Govindaiah Vinukonda,[1] Anna Csiszar,[2] Furong Hu,[1] Krishna Dummula,[1] Nishi Kant Pandey,[1] Muhammad T. Zia,[1] Nicholas R. Ferreri,[3] Zoltan Ungvari,[2] Edmund F. LaGamma[1] and Praveen Ballabh[1,4]

1 Department of Paediatrics, New York Medical College-Westchester Medical Centre, Valhalla, NY 10595, USA
2 Reynolds Oklahoma Center on Aging, University of Oklahoma Health Sciences Center, Oklahoma City, OK 73104
3 Department of Pharmacology, New York Medical College-Westchester Medical Centre, Valhalla, NY 10595, USA
4 Department of Anatomy and Cell Biology, New York Medical College-Westchester Medical Centre, Valhalla, NY 10595, USA

Correspondence to: Praveen Ballabh,
Regional Neonatal Centre,
2nd floor, Maria Fareri Children's Hospital at Westchester Medical Centre,
Valhalla,
NY 10595, USA
E-mail: pballabh@msn.com

Intraventricular haemorrhage is a major complication of prematurity that results in neurological dysfunctions, including cerebral palsy and cognitive deficits. No therapeutic options are currently available to limit the catastrophic brain damage initiated by the development of intraventricular haemorrhage. As intraventricular haemorrhage leads to an inflammatory response, we asked whether cyclooxygenase-2, its derivative prostaglandin E2, prostanoid receptors and pro-inflammatory cytokines were elevated in intraventricular haemorrhage; whether their suppression would confer neuroprotection; and determined how cyclooxygenase-2 and cytokines were mechanistically-linked. To this end, we used our rabbit model of intraventricular haemorrhage where premature pups, delivered by Caesarian section, were treated with intraperitoneal glycerol at 2 h of age to induce haemorrhage. Intraventricular haemorrhage was diagnosed by head ultrasound at 6 h of age. The pups with intraventricular haemorrhage were treated with inhibitors of cyclooxygenase-2, prostanoid receptor-1 or tumour necrosis factor-α; and cell-infiltration, cell-death and gliosis were compared between treated-pups and vehicle-treated controls during the first 3 days of life. Neurobehavioural performance, myelination and gliosis were assessed in pups treated with cyclooxygenase-2 inhibitor compared to controls at Day 14. We found that both protein and messenger RNA expression of cyclooxygenase-2, prostaglandin E2, prostanoid receptor-1, tumour necrosis factor-α and interleukin-1β were consistently higher in the forebrain of pups with intraventricular haemorrhage relative to pups without intraventricular haemorrhage. However, cyclooxygenase-1 and prostanoid receptor 2–4 levels were comparable in pups with and without intraventricular haemorrhage. Cyclooxygenase-2, prostanoid receptor-1 or tumour necrosis factor-α inhibition reduced inflammatory cell infiltration, apoptosis, neuronal degeneration and gliosis around the ventricles of pups with intraventricular haemorrhage. Importantly, cyclooxygenase-2 inhibition alleviated neurological impairment, improved myelination and reduced gliosis at 2 weeks of age. Cyclooxygenase-2 or prostanoid receptor-1 inhibition reduced tumour necrosis factor-α level, but not interleukin-1β. Conversely, tumour necrosis factor-α

Received September 20, 2009. Revised March 14, 2010. Accepted April 5, 2010. Advance Access publication May 20, 2010

antagonism did not affect cyclooxygenase-2 expression. Hence, prostanoid receptor-1 and tumour necrosis factor-α are downstream to cyclooxygenase-2 in the inflammatory cascade induced by intraventricular haemorrhage, and cyclooxygenase-2-inhibition or suppression of downstream molecules—prostanoid receptor-1 or tumour necrosis factor-α—might be a viable neuroprotective strategy for minimizing brain damage in premature infants with intraventricular haemorrhage.

Keywords: cyclooxygenase-2; prostanoid receptor; germinal matrix haemorrhage; intraventricular haemorrhage; premature rabbit pups; tumour necrosis factor-alpha; celecoxib

Abbreviations: COX-2 = cyclooxygenase-2; EP = prostanoid receptor; GFAP = glial fibrillary acidic protein; IL-1β = interleukin-1β; IVH = intraventricular haemorrhage; PBS = phosphate buffered saline; PCR = polymerase chain reaction; PGE2 = prostaglandin E2; TNF-α = tumour necrosis factor-alpha; TUNEL = terminal deoxynucleotidyl transferase dUTP nick end labelling

Introduction

Germinal matrix haemorrhage-intraventricular haemorrhage (IVH) occurs in about 12 000 premature infants every year in the USA, and predisposes the survivors to cerebral palsy and cognitive deficits (Heuchan *et al*., 2002). IVH is not substantially preventable and the treatment of the resultant brain injury is non-existent. The development of IVH results in an inflammatory response, oxidative stress and neural cell death, predominantly around the lateral ventricles of the forebrain (Georgiadis *et al*., 2008; Zia *et al*., 2009). Cyclooxygenase 2 (COX-2)—an inducible enzyme catalyzing synthesis of prostanoid—plays a key role in cerebral pathologies associated with inflammation, oxidative injury and glutamate excitotoxicity (FitzGerald, 2003; Minghetti, 2007). Therefore, we asked whether COX-2 derived prostanoids contribute to IVH-induced brain injury in premature newborns and if so, whether inhibition of COX-2 or its downstream mediators would offer neuroprotection.

COX-2 expression is markedly upregulated in a wide range of brain diseases including traumatic, ischaemic and degenerative diseases, and inhibition of this enzyme confers neuroprotection in animal models of brain injury (Chu *et al*., 2004; Gopez *et al*., 2005). Accordingly, celecoxib, a COX-2 inhibitor, reduces cerebral inflammation and brain oedema and facilitates functional recovery in rat model of hypoxia-ischaemia (Chu *et al*., 2004). Emerging evidence indicates that prostaglandin E2 (PGE2) mediates neuro-toxicity of COX-2 (Cimino *et al*., 2008). PGE2 activates G-protein coupled receptors, including prostanoid receptor (EP)1, EP2, EP3 and EP4. Activation of EP1 elicits neurotoxicity while EP2, EP3 and EP4 are neuro-protective (Bilak *et al*., 2004; Ahmad *et al*., 2005). Indeed, gene inactivation or pharmacological blockade of EP1 provides neuroprotection in models of excitotoxicity, cerebral-ischaemia and oxygen glucose deprivation (Kawano *et al*., 2006).

IVH results in an inflammatory response consisting of cell death, microglia infiltration and gliosis (Georgiadis *et al*., 2008). Activated microglia and reactive astrocytes produce pro-inflammatory cytokines—tumour necrosis factor-alpha (TNF-α) and interleukin-1β (IL-1β), which are associated with neonatal cerebral-injuries (Kaur and Ling, 2009). Importantly, several studies demonstrate a regulatory cross-talk between COX-2 and TNF-α pathways (Ikawa *et al*., 2001; Martinet *et al*., 2009). COX-2 inhibition suppresses TNF-α production in neuronal-glial culture experiments and alleviates the cellular inflammatory response in a rat stroke model (Brambilla *et al*., 1999; Araki *et al*., 2001; Ahmad *et al*., 2009). Conversely, pharmacological inhibition of TNF-α suppresses COX-2 levels in an *in vitro* model of peritoneal macrophages (Crisafulli *et al*., 2009; Martinet *et al*., 2009). Thus, it is important to determine how COX-2, prostanoid receptors, pro-inflammatory cytokines, cell death and gliosis are mechanistically linked in the signalling cascade in order to develop an optimal therapeutic strategy for IVH. On this basis, we hypothesized that COX-2, its derivative PGE2, EP1 receptor and pro-inflammatory cytokines (TNF-α and IL-1β) might be elevated in preterm newborns with IVH, and that inhibitors of COX-2, EP1 receptor or TNF-α would attenuate inflammation, neuronal cell death and gliosis, thereby offering neuroprotection. We also postulated that COX-2 or EP1 receptor inhibition might reduce pro-inflammatory cytokines, and that TNF-α inhibition would suppress COX-2 levels.

To test our hypotheses, we adopted our rabbit pup (E29, term = 32 days) model of IVH, as this model mimics preterm infants with IVH (Ballabh *et al*., 2007; Georgiadis *et al*., 2008). The present study revealed that IVH resulted in upregulation of COX-2, TNF-α, IL-1β and EP1, but not EP2-4. Suppression of COX-2, EP1 or TNF-α offered neuroprotection. Furthermore, EP1 and TNF-α are downstream to COX-2 in the signalling cascade induced by IVH. Hence, the present study identifies a novel strategy for neuroprotection in premature newborns with IVH and substantially unravels the mechanistic links not only between the three interwoven molecules—COX-2, EP1 and TNF-α—but their relation to cell death and gliosis in brain haemorrhage of premature infants.

Materials and methods

Animal experiment

The Institutional Animal Care and Use Committee of New York Medical College approved the animal protocol. The details of brain injuries in our model of glycerol-induced IVH have been previously established and published (Georgiadis *et al*., 2008; Chua *et al*., 2009). We obtained timed pregnant New Zealand rabbits from Charles River Laboratories, Inc. (Wilmington, MA, USA). We delivered the pups prematurely by Caesarean section at E29 (full-term = 32 days). Pups were dried and kept in an infant incubator pre-warmed to a temperature of 35°C. Pups were fed 1 ml rabbit milk at 4 h of age

and then ~2 ml every 12 h (100 ml/kg/day) for the first 2 days using 3.5 French feeding tube. After Day 2, we used kitten milk formula (KMR, PETAG Inc. IL, USA) and advanced feeds to 125, 150, 200, 250 and 280 ml/kg on postnatal Days 3, 5, 7, 10 and 14, respectively.

At 2 h of age, we treated rabbit pups with 50% glycerol (6.5 g/kg) intraperitoneally to induce IVH. Head ultrasound was performed at 6 h of age to assess the presence and severity of IVH using an Acuson Sequoia C256 (Siemens) ultrasound machine. IVH was classified as (i) mild, no gross signs but microscopic haemorrhage detected in haematoxylin and eosin stained brain sections; (ii) moderate, gross haemorrhage into lateral ventricles (two separate lateral ventricles discerned); or (iii) severe, gross IVH leading to fusion of lateral ventricles into a common chamber (Chua *et al*., 2009). About 80% of rabbit pups develop moderate-severe IVH and 15% mild IVH after glycerol treatment (Georgiadis *et al*., 2008). As microscopic IVH cannot be diagnosed by head ultrasound, a diagnosis of absence of IVH in glycerol-treated pups indicates that the kit had either microscopic haemorrhage or no IVH. To evaluate the effect of haemorrhage on parameters (COX-2, EP1, TNF-α, IL-1β or Caspase activity), we included three groups of pups: (i) glycerol-induced IVH; (ii) glycerol-induced non-IVH (control); and (iii) saline treated non-IVH (control). Inclusion of two control groups determined whether intraperitoneal glycerol treatment would confound the IVH-induced morphological (cell infiltration and death) and molecular changes (COX, cytokines) in the forebrain. Accordingly, our previous study had shown that there was no significant cell death or cellular infiltration in the forebrain of glycerol-treated non-IVH pups, just as in saline-treated non-IVH pups (Georgiadis *et al*., 2008). To assess the effect of treatment (celecoxib/SC51089/etanercept), we alternately assigned pups with moderate-to-severe haemorrhage (glycerol-induced) into two groups—treatment group and vehicle controls. We confirmed that the two groups were balanced with respect to the severity of IVH.

Celecoxib, SC51089 or etanercept treatment

To suppress COX-2, we treated pups with subcutaneous celecoxib (Pfizer Inc., 20 mg/kg/day once daily for 3 days). For evaluation of long-term outcome, we treated the pups with subcutaneous celecoxib for 7 days (20 mg/kg/day once daily) starting at Day 1 and performed neurological and histochemical evaluation at Day 14. To block EP1, we treated another subset of pups with SC-51089 {8-chlorodibenz [b,f][1,4]oxazepine-10(11H)- carboxylic acid, 2-[1-oxo-3-(4-pyridinyl) propyl] hydrazide hydrochloride; Sigma, St Louis, MO; 10 mg/kg twice daily for 3 days}. TNF-α was inhibited by using intracerebroventricular etanercept (Amgen and Wyeth pharmaceuticals, CA, USA; 2 mg/kg diluted to 20 µl once in both lateral ventricles). To assess the effect of COX-2, EP1 or TNF-α inhibitors, pups with IVH were alternatively assigned at 6 h age to receive either the compound or the vehicle (control). The severity of IVH was comparable between the comparison groups. Etanercept was injected into the cerebral ventricle using the following coordinates from Bregma: 1 mm posterior, 4 mm lateral and 3 mm deep. We used a 30 gauge needle mounted on Hamilton syringe for drug administration. The doses of these medications were based on previous studies (Chu *et al*., 2004; Kawano *et al*., 2006; Tobinick and Gross, 2008).

Rabbit tissue collection and processing

We processed the tissues as described previously (Ballabh *et al*., 2007). The brain slices were immersion-fixed in 4% paraformaldehyde in phosphate buffered saline (PBS; 0.01 M, pH 7.4) for ~18 h and then were cryoprotected by immersing into 20% sucrose in 0.01 M PBS for 24 h followed by 30% sucrose for the next 24 h. Tissues were frozen into optimum cutting temperature compound (Sakura, Japan). Frozen coronal blocks were cut into 12 µm sections using cryostat.

Immunohistochemistry

Immunostaining was performed as described before (Ballabh *et al*., 2007). The primary antibodies used in experiments included goat polyclonal COX-2 (Catalogue #160112, Caymen Chemicals, MI, USA), goat polyclonal COX-1 (Catalogue # sc 1752; Santa Cruz, CA, USA), goat polyclonal TNF-α (sc-1350, Santa Cruz, CA, USA), mouse monoclonal glial fibrillary acidic protein (GFAP) (Catalogue #G3893, St Louis, MO, USA), monoclonal mouse anti-rabbit neutrophil (Catalogue #801, Serotec, NC, USA), monoclonal mouse anti rabbit CD11b (Catalogue #MCA802, Serotec, NC, USA) and rat monoclonal myelin basic protein (Catalogue # 7349, Abcam, MA). The secondary antibodies used were Cy-3 conjugate goat anti-mouse and fluorescein isothiocyanate conjugate goat anti-rat (Jackson Immunoresearch, West Grove, PA, USA). Briefly, fixed sections were hydrated in 0.01 M PBS and incubated with the primary antibodies diluted in PBS overnight at 4°C. After washing in PBS, the sections were incubated with secondary antibody diluted in 1% normal goat serum in PBS at room temperature for 60 min. Finally, after washes in PBS, sections were mounted with Slow Fade Light Antifade reagent (Molecular Probes, Invitrogen, CA, USA) and were visualized under fluorescent microscope (Axioscope 2 Plus, Carl Zeiss, Inc. Germany).

Neuronal degeneration and fluorescent *in situ* detection of DNA fragmentation

We performed Fluro-Jade (Chemicon) and terminal deoxynucleotidyl transferase dUTP nick end labelling (TUNEL) staining on fixed brain sections as described previously (Georgiadis *et al*., 2008). For TUNEL staining, 15 µm tissue sections were air dried on slides, hydrated in 0.01 M PBS and permeabilized for 5 min in 1:1 ethanol:acetic acid. An ApopTag-fluorescein *in situ* DNA fragmentation detection kit (Chemicon, CA, USA) was used to visualize TUNEL-labelled nuclei.

Quantification of cell infiltration, death, gliosis and myelination

We counted neutrophil, microglia, TUNEL positive nuclei, degenerated neurons and astrocytes in coronal brain sections of treatment (celecoxib, SC51089 or etanercept) pups with IVH compared with vehicle-treated IVH controls. From each brain, six coronal sections (30 µm) taken as every third section at the level of midseptal nucleus were used for the study. Counting was performed in an unbiased fashion and random basis in the periventricular zone (germinal matrix, caudate nucleus, deep corona radiata and corpus callosum around the ventricle) and the cerebral cortex by two blinded investigators using a fluorescent microscope with 40× objective (Zeiss Axioscope 2 plus, Carl Zeiss Inc, Germany). We counted objects in ~120 images (7–10 images × two brain regions × six coronal sections) per brain ($n = 5$ pups per each group) for each parameter.

To evaluate myelination, we analysed images acquired from corona radiata and corpus callosum of brain sections double labelled with myelin basic protein and panaxonal filament antibodies, as previously described (Chua *et al*., 2009). We used Metamorph version 6.1 from

Universal Imaging Corporation 1993–2003 (Downington, PA). The two sources of image, myelin basic protein (red) and panaxonal filament (green), were displayed on the Metamorph screen. Both images were thresholded. The software calculated the percentage overlap of red (myelin basic protein) over green signal (panaxonal filament). We compared images from non-IVH, vehicle-treated IVH and celecoxib-treated IVH pups ($n = 5$ pups each).

Western blot analyses

The frozen brain tissue was homogenized in sample buffer (3% sodium dodecyl sulphate, 10% glycerol, 62.5 mM Tris–HCl and 100 mM Dithiothreitol) using a mechanical homogenizer and the samples were boiled immediately for 5 min. The protein concentration in the sample was determined using RC–DC Protein Assay Kit (Biorad, CA, USA) and dilutions of bovine serum albumin were used as the standard. Total protein samples were separated by sodium dodecyl sulphate–polyacrylamide gel electrophoresis according to the previously described method (Laemmli *et al*., 1970). Equal amounts of protein (30 μg) were loaded into 4–15% gradient precast gel (Biorad, CA, USA). The separated proteins were transferred to polyvinylidene difluoride membrane by electrotransfer. The membranes were then incubated with primary antibodies. Target proteins were detected with enhanced chemiluminescence system (ECL system; Amersham) by using secondary antibodies conjugated with horseradish peroxidase (Jackson immunoresearch, PA, USA). The blots were then stripped with stripping buffer (Pierce) and incubated with β actin primary antibody followed by secondary antibody and detection with ECL system. As described previously (Ballabh *et al*., 2007), the blots from each experiment were densitometrically analysed using J-image. We used pre-calibrated optical density step tablet to calibrate an image J (rsbweb.nih.gov/ij/) and then measured the optical density of the bands. The optical density values were normalized by taking the ratio of the target protein and β actin. The antibodies used for immunohistochemsitry and western blot analyses were the same for each parameter; except in the GFAP western blot when we used mouse monoclonal GFAP from BD biosciences (Catalog # 556327).

Quantitative real-time polymerase chain reaction

Quantitative real-time polymerase chain reaction (PCR) was performed as described previously (Braun *et al*., 2007). Briefly, total RNA was isolated from a 1 mm thick slice taken at the level of mid-septal nucleus of the forebrain using Mini RNA Isolation Kit (Zymo Research, CA). RNA was reverse-transcribed using Superscript II RT (Invitrogen, CA). Real-time reverse transcription PCRs were used to analyse mRNA expression using the Stratagene MX3000, GmbH (Bernried, Germany). Quantification was performed using the efficiency-corrected ΔΔCT method. The following primers were used for quantitative real-time PCR: (i) COX-2 (Accession #U97696): 5-CACTGATGGGCTGTTTTCT TAG-3′ (sense), 5′-CCGACTTGGTTCCGATGC-3′ (antisense); (ii) COX-1 (Accession #AF026008): 5′-AACCTAATGCCCAACAAG-3′ (sense), 5′-TCTAAGTGGACAAGAATACC-3′ (antisense); (iii) EP1 (Accession #AF043491): 5′-TTGTCGGTATCATGGTGGTGTCGT-3′ (sense), 5′-ATGTACACCCAAGGGTCCAGGAT-3′ (antisense); (iv) EP2 (Accession #AY166779): 5′-GACCCTCTTCCTCCCAGGTAAAGG-3′ (sense), 5′-TCAGACTGGGAGTCATTGGAGGCATT-3′ (antisense); (v) EP3 (Accession #AK315825): 5′-ACTGGTATGCGAGCCACATGA AGA-3′ (sense), 5′-GTTATGCGAAGAGCTAGTCCCGTT-3′ (antisense); (vi) EP4 (Accession #L47207): 5′-TACCTGGCCATCAACCATGC CTAT-3′ (sense), 5′-AAGAGCACGTTGGACGCATAGACT-3′ (antisense); (vii) IL-1β (Accession #M26295): 5′-AAGAAGAACCCGT CCTCTGCAACA-3′ (sense), 5′-TCAGCTCATACGTGCCAGACAACA-3′ (antisense); and (viii) TNF-α (Accession #NM_001082263): 5′-ATGGT CACCCTCAGATCAGCTTCT-3′ (sense), 5′-AAGAGAACCTGGGAGT AGATGAGG-3′ (antisense).

Prostaglandin E2 assay

Rabbit pup brain tissue was weighed, snap frozen and stored at –80°C until use. Frozen tissues were homogenized using a Polytron (Brinkman) in 100% methanol, centrifuged and the supernatants were collected, dried under a stream of nitrogen, resuspended in 500 μl of enzyme immunoassay buffer and subsequently assayed for PGE2 by enzyme immunoassay (Cayman Chemical, Ann Arbor, MI).

Caspase-Glo assay

We used the Caspase-Glo R 3/7, 8 and 9 Assay Kit (Promega, catalogue #G8091, G8201 and G8211) to measure their activity in the tissue. Briefly, forebrain extracts made in extraction buffer (25 mM HEPES, pH 7.5, 5 mM $MgCl_2$, 1 mM EGTA, 1 mM Pefabloc and 1 Ug/ml each pepstatin, leupeptin and aprotinin) were treated with luminogenic caspase substrate and luminometre readings were taken at 1 h.

Neurobehavioural assessment

We performed neurobehavioural testing at postnatal Day 14 based on the scoring protocol described previously (Derrick *et al*., 2004; Georgiadis, 2008; Chua *et al*., 2009). The evaluation was performed by two physicians blinded to group assignment. We examined cranial nerves by testing smell (aversive response to ethanol), sucking and swallowing (formula delivered by a plastic pipette). We graded the responses on a scale of 0–3, 0 being the worst response and 3 the best. Motor evaluation included tone (modified Ashworth's scale), motor activity, locomotion at 30° angle, righting reflex and gait. Tone was examined by active flexion and extension of forelegs and hindlegs (score 0–3). The righting reflex was assessed by ability and rapidity to turn prone when placed in supine position. Sensory examination included touch on face (touching face with cotton swab) and extremities as well as pain on limbs (mild pin prick). Grading of tone, gait and locomotion at 30° angle are illustrated in the footnote of Table 1. To assess coordination and muscle strength in fore and hindlegs, we evaluated the ability of the pups to hold their position on a 60° slope. The test was conducted on a rectangular surface (18 × 6 inch) kept at 60° inclination. We placed the pup at the upper end of the inclination and measured the latency to slip down the slope. We preformed the visual cliff test for the assessment of vision. All animals could detect the cliff.

Statistics and analysis

Data are expressed as mean and SEM. The parameters were compared between pups with and without IVH as well as a function of postnatal age 12, 48 and 72 h. We used *t*-test (parametric variable) or Mann–Whitney *U*-test (non-parametric variable) to perform pairwise comparison and ANOVA to compare multiple groups. A probability value of 0.05 was considered significant.

Table 1 Neurobehavioural evaluation of premature pups (E29) at postnatal Day 14

System	Test	Glycerol-treated pups without IVH, $n=17$	Glycerol-treated pups with IVH, vehicle-treated, $n=17$	Glycerol-treated pups with IVH, celecoxib-treated, $n=16$
Cranial nerves	Aversive response to alcohol	3 (3,3)	3 (3,3)	3 (3,3)
	Sucking and swallowing	3 (3,3)	3 (3,3)	3 (3,3)
	Vision	3 (3,3)	3 (3,3)	3 (3,3)
Motor	Motor activity			
	Head	3 (3,3)	3 (3,3)	3 (3,3)
	Forelegs	3 (3,3)	3 (3,3)	3 (3,3)
	Hind legs	3 (3,3)	3 (2.7,3)	3 (3,3)
	Righting reflex[a]	5 (5,5)	5 (4,5)	5 (4,5)
	Locomotion on 30° inclination[b]	3 (3,3)	3 (3,3)	3 (3,3)
	Tone[c]	0 (0,0)	0 (0,0)	0 (0,0)
	Forelimb	0 (0,0)	0 (0,0)	0 (0,0)
	Hindlimb			
	Hold their position at 60° inclination (latency to slip down the slope in seconds)	12.0	7.1	$14.7^{###}$
	Distance walked in 60 s (in inches)	96	66	$85^{#}$
Gait[d]		4 (4,4)	3 (2.75–3.25)	$4\ (3,4)^{#}$
Motor impairment	Weakness in extremities (%)	0%	23.52%	6.25%
Sensory	Facial touch	3 (3,3)	3 (3,3)	3 (3,3)
	Pain	3 (3,3)	3 (3,3)	3 (3,3)

Values are median and interquartile range. 0 is the worst response and 3 is the best response.

a Score (range 1–5): number of times turns prone within 2 s when placed in supine out of 5 tries.

b Score (range 0–3): 0 = does not walk; 1 = takes a few steps (less than 9 inches); 2 = walks for 9–18 inches; 3 = walks very well beyond 18 inches.

c Score (range 1–3): 0 = no increase in tone; 1 = slight increase in tone; 2 = considerable increase in tone; 3 = limb rigid in flexion or extension.

d Gait was graded as 0 (no locomotion), 1 (crawls with trunk touching the ground for few steps and then rolls over), 2 (walks taking alternate steps, trunk low and cannot walk on inclined surface), 3 (walks taking alternate steps, cannot propel its body using synchronously the hind legs, but walks on 30° inclined surface), 4 (walks, runs, and jumps without restriction, propels the body using synchronously the backlegs, but limitation in speed, balance, and coordination manifesting as clumsiness in gait), or 5 (normal walking).

$^{#}P<0.05$, $^{###}P<0.001$ for the comparison between celecoxib-treated and vehicle-treated pups with IVH. Mann–Whitney *U*-test used.

Results

Induction of COX-2 and PGE2 after intraventricular haemorrhage, but not COX-1

Since COX-2 is upregulated in hypoxia-ischaemic, traumatic and degenerative brain injuries, and as COX-2 activation exacerbates tissue damage (FitzGerald, 2003; Minghetti, 2007), we asked whether COX-2 expression was enhanced in the forebrain of premature animals with IVH. To this end, we injected glycerol intraperitoneally to induce IVH in premature rabbit pups (E29) at 2 h of age and performed head ultrasound at 6 h of age to determine the presence and severity of IVH (Supplementary Fig. 1A). We evaluated COX-2 expression by immunohistochemistry, western blot analysis and real-time PCR in the forebrain of pups with and without IVH at 12, 48 and 72 h of postnatal age. Immunohistochemistry revealed that COX-2 was abundantly expressed in immature neurons and moderately to weakly in astrocytes and microglia, located around the lateral ventricle (periventricular zone, including germinal matrix, deep white matter and caudate nucleus) of pups with IVH (Fig. 1A and Supplementary Fig. 1B and C). By contrast, COX-2 was weakly expressed in the neuronal and glial cells of the periventricular zone of pups without IVH. COX-2 immunoreactivity was weak in the cerebral cortex of both pups with and without IVH. Western blot analysis confirmed that COX-2 levels were higher in pups with IVH than in glycerol-treated controls without IVH at all three epochs—12, 48 and 72 h postnatal age ($P=0.02$, 0.01 and 0.02, respectively, $n=8$ per group at each time point, Fig. 1B). Similarly, real time PCR revealed that COX-2 mRNA expression was greater in pups with IVH compared to saline- and glycerol-treated controls without IVH at 12, 48 and 72 h postnatal age ($P<0.05$ each, $n=6$ per group at each time point, Fig. 1C). In contrast, both mRNA and protein expression of COX-1 were comparable between pups with IVH and controls without IVH at all the three epochs—12, 48 and 72 h of postnatal age ($n=8$ per group at each time point) (Fig. 1D and E).

PGE2 is a COX-2 derivative and mediates neurotoxicity through prostanoid receptors (Kawano *et al.*, 2006). It was, therefore, important to determine whether IVH enhanced PGE2 levels. PGE2 levels, in homogenates made from coronal slice taken at the level of mid-septal nucleus, were significantly higher in pups with IVH compared to glycerol-treated controls without IVH at both 12 h (39.2 ± 11.8 versus 12.2 ± 3.2 ng/g, $n=8$ each, $P<0.05$) and 48 h (18.4 ± 3.4 versus 6.7 ± 0.9 ng/g, $n=8$ each, $P<0.05$) of age. In conclusion, the development of IVH was associated with upregulation of COX-2 and PGE2 synthesis, while levels of COX-1 remained the same.

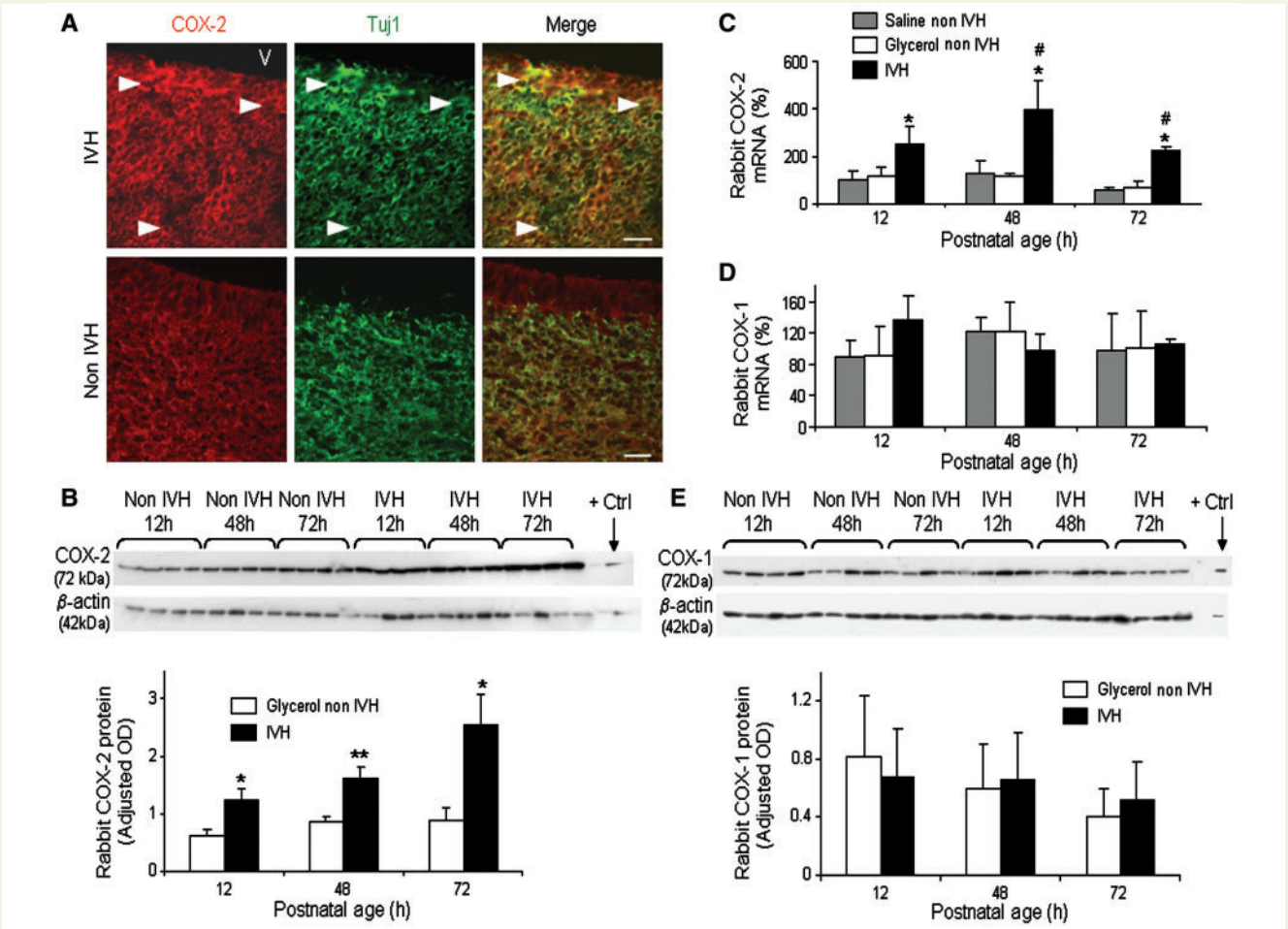

Figure 1 Greater COX-2 expression in premature rabbit pups with IVH compared to controls. (**A**) Representative immunofluorescence of cryosections from periventricular germinal matrix of premature rabbit pup (E29) with and without IVH double-labelled with COX-2 and Tuj1 (β tubulin) specific antibodies. COX-2 expression was substantially stronger in the germinal matrix of pups with IVH compared to pups without IVH. COX-2 immunoreactivity co-localized with Tuj 1 positive neurons. Scale bar, 20 μm. V = ventricle. (**B**) Western blot analyses for COX-2 in the forebrain of premature rabbit pups with and without IVH at 12, 48 and 72 h of age. HeLa cell lysate used as positive control. The bar diagram shows mean ± SEM ($n = 8$ per group at each time point). Values were normalized to β-actin. The COX-2 levels were higher in the forebrain of premature pups with IVH compared to controls without IVH at each of the three epochs. COX-2 levels significantly increased as a function of postnatal age in pups with IVH. $^{*}P < 0.05$ and $^{**}P < 0.01$ for IVH versus non-IVH at each time point. (**C**) *COX-2* mRNA expression assayed by real time PCR in the forebrain of premature pups with and without IVH at 12, 48 and 72 h of age. Data are mean ± SEM ($n = 6$ per group at each time point). *COX-2* expression was significantly higher in the pups with IVH compared to the saline- and glycerol-treated controls without IVH at each of the three epochs. $^{*}P < 0.05$ for pups with IVH versus saline-treated controls without IVH; $^{\#}P < 0.05$ for pups with IVH versus glycerol-treated controls without IVH. (**D**) A time-course changes of *COX-1* gene expression, measured by real time PCR, in the forebrain of pups with and without IVH at 12, 48 and 72 h of age. Data are mean ± SEM ($n = 6$ per group at each time point). There was no significant difference in COX-1 mRNA level between pups with and without IVH at any of the epochs. (**E**) Representative western blot analysis for COX-1 protein in the forebrain of pups with and without IVH at 12, 48 and 72 h of age. COL0320 DM cell lysate (Santa Cruz) was used as a positive control. The bar diagram shows mean ± SEM ($n = 8$ per group at each time point). The data were normalized to β-actin. COX-1 protein levels in pups with and without IVH were similar at each of the three time points. OD = optical density.

Celecoxib suppresses PGE2, cellular infiltration, cell death and gliosis in pups with intraventricular haemorrhage

Since COX-2 contributes to an inflammatory response (Minghetti, 2007), we next postulated that COX-2 inhibition could suppress PGE2 and inflammation in pups with IVH. To this end, we alternately assigned pups with glycerol-induced IVH (detected by head ultrasound) to receive either subcutaneous celecoxib (20 mg/kg/day once daily for 3 days) or vehicle (30 μl dimethyl sulphoxide) at 6 h of age. The severity of IVH was comparable between the treatment and control (vehicle) pups. PGE2 levels were significantly reduced in treated pups compared to vehicle controls at both 12 and 48 h of age ($P = 0.01$ and 0.04, respectively, $n = 8$

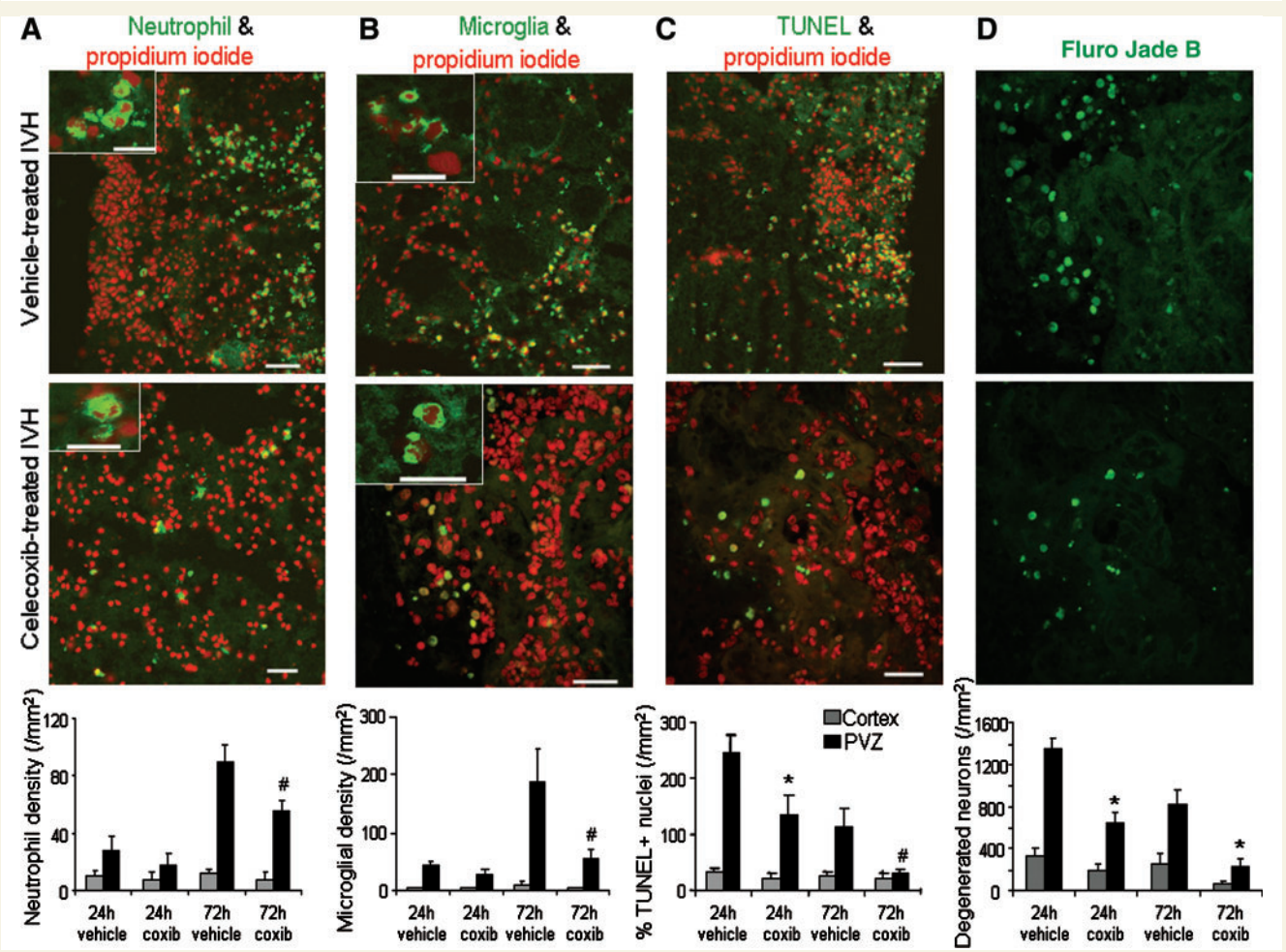

Figure 2 Reduced cell infiltration and cell death in celecoxib-treated pups with IVH compared to controls. (**A**) Representative immunofluorescence of cryosections immunolabelled with rabbit neutrophil specific antibody and propidium iodide (nuclear stain). The section is from the periventricular zone of pups with IVH that were treated with either celecoxib (lower panel) or vehicle (upper panel). Neutrophils were few in celecoxib-treated pups with IVH and abundant in vehicle-treated pups with IVH. Inset shows neutrophil labelling under high magnification. Data for neutrophil count are depicted as mean ± SEM ($n = 5$ per group at each time point). Neutrophil count in the periventricular zone was significantly lesser in celecoxib-treated pups with IVH compared to controls at 72 h of age, but not at 24 h. (**B**) Cryosections from forebrain of celecoxib-treated and vehicle-treated pups with IVH were labelled with CD11b specific antibody and propidium iodide. CD11b positive microglia were scarce in the brain region around the ventricles in celecoxib-treated pups with IVH, but numerous in vehicle-treated controls. Inset shows microglia labelling under high magnification. Data are mean ± SEM ($n = 7$ per group at each time point). CD11b positive microglia were significantly lower in density in the periventricular zone of celecoxib-treated pups with IVH compared to vehicle controls at 72 h of age, but not at 24 h. In the cerebral cortex, microglial density was similar in celecoxib-treated pups and vehicle controls. (**C**) Representative TUNEL labelling of the periventricular zone from pups with IVH that were treated with either celecoxib or vehicle. The section was counterstained with propidium iodide. TUNEL positive nuclei were less abundant in celecoxib-treated pups compared to vehicle controls. Data are mean ± SEM ($n = 5$ per group at each time point). TUNEL positive nuclei were lesser in number in celecoxib-treated pups with IVH compared to vehicle controls at both 24 and 72 h of age. Apoptotic nuclei were similar in density in the cerebral cortex of celecoxib-treated pups and vehicle controls. (**D**) Rabbit pups with IVH were treated with either celecoxib or vehicle. Cryosections were stained with FluorJadeB. Data are mean ± SEM ($n = 7$ per group at each time point). Degenerated neurons were lesser in density in celecoxib-treated pups with IVH compared to vehicle controls at both 24 and 72 h of age. However, the degenerated neurons were similar in density in the cerebral cortex of celecoxib-treated pups and vehicle controls. $^{*}P < 0.05$ for celecoxib treated pups with IVH versus vehicle treated controls at 24 h; $^{\#}P < 0.05$ for celecoxib-treated pups with IVH versus vehicle controls at 72 h. All scale bars = 20 μm. Coxib = celecoxib treatment; PVZ = periventricular zone.

each, data not shown). We then assessed the density of neutrophils and microglia in the periventricular zone and cerebral cortex of treated pups and vehicle controls. The neutrophil density was diminished in the periventricular zone at 72 h ($P = 0.045$, $n = 5$ each), but not at 24 h of age, in celecoxib-treated pups with IVH compared to vehicle controls (Fig. 2A). Likewise, microglial density was reduced in the periventricular zone of celecoxib-treated pups compared to vehicle controls at 72 h ($P = 0.027$,

$n = 7$ each, Fig. 2B), but not at 24 h of age. In the cerebral cortex, neutrophil and microglial density were similar between treated pups and vehicle controls.

Since celecoxib treatment reduced cellular infiltration around the ventricle, we next assessed cellular death in celecoxib-treated pups with IVH relative to vehicle-treated controls with IVH at 24 and 72 h postnatal age. We performed TUNEL staining for the evaluation of apoptosis and Fluoro Jade B labelling for the assessment of neuronal degeneration. We noted lower density of TUNEL positive nuclei in the periventricular zone of celecoxib-treated pups compared to vehicle controls at both 24 and 72 h of age ($P = 0.03$ and 0.045, $n = 5$ each, Fig. 2C). Likewise, neuronal degeneration was reduced in the periventricular zone of celecoxib-treated pups relative to vehicle controls at both 24 and 72 h of age ($P < 0.016$ and 0.014, $n = 7$ each, Fig. 2D). In the cerebral cortex, neuronal degeneration and apoptosis were comparable between treatment group and vehicle controls.

IVH results in gliosis (Chua *et al*., 2009) and PGE2, a COX-2 derivative, is considered a key mediator of gliosis (Hwang *et al*., 2006). Thus, we compared gliosis in celecoxib-treated pups with IVH and vehicle-treated controls with IVH. We observed only few hypertrophic astrocytes—with relatively large cell bodies and several processes making a dense network—in the periventricular zone of celecoxib-treated pups, but these were abundant in vehicle controls. Accordingly, astrocyte counts confirmed that there were fewer GFAP positive astroglial cells in the periventricular zone of celecoxib-treated pups than in vehicle controls at 72 h of age ($P < 0.001$, $n = 6$ each) (Supplementary Fig. 2A). We then quantified GFAP protein in the forebrain of glycerol-treated pups without IVH, untreated pups with IVH and celecoxib-treated pups with IVH by western blot analyses. Consistent with immunohistochemical data, GFAP protein level was significantly elevated in pups with IVH compared to controls without IVH ($P < 0.01$) and more importantly, celecoxib treatment substantially reduced GFAP level in pups with IVH ($P < 0.01$, $n = 5$, Supplementary Fig. 2B). In conclusion, celecoxib treatment reduced PGE2 synthesis, cellular infiltration, cell death and gliosis around the lateral ventricle of pups with IVH, and thus, conferred neuroprotection.

Celecoxib attenuates elevation of caspase-3/7, -8 and -9 in intraventricular haemorrhage

IVH may trigger both the intrinsic and extrinsic pathways of apoptosis (Broughton *et al*., 2009). Therefore, we compared caspase-3/7 (effector caspase), -8 and -9 activities among the forebrains of (i) saline-treated pups without IVH; (ii) glycerol-treated pups without IVH; (iii) vehicle-treated pups with IVH; and (iv) celecoxib-treated pups with IVH, at 12, 48 and 72 h postnatal age.

Expression of all three caspases were significantly higher in pups with IVH compared to saline- and glycerol-treated pups without IVH ($P < 0.001$ all, $n = 6$ each). Caspase-3/7 and -9 activity were reduced in celecoxib-treated pups compared to vehicle controls at 12 h ($P < 0.004$ and 0.008 for caspase-3/7 and -9, respectively) and 48 h ($P = 0.02$, 0.03, respectively), but not at 72 h ($P = 0.3$, 0.07, respectively, $n = 6$ each) (Supplementary Fig. 3). Of note, capsase-8 activity was significantly less in celecoxib-treated pups with IVH compared to vehicle-treated controls with IVH at 12, 48 and 72 h of age ($P = 0.004$, 0.02, 0.012, respectively, $n = 6$ each). In conclusion, IVH induced both intrinsic and extrinsic pathways of apoptosis and celecoxib treatment suppressed both the cascades.

COX-2 inhibition suppresses EP1 in pups with intraventricular haemorrhage and EP1 inhibition offers neuroprotection

Since PGE2 acts through EP receptors (EP1-4) (Alvarez-Soria *et al*., 2007), we chose to (i) compare the expression of EP1-4 receptor between pups with and without IVH; and (ii) determine the effect of COX-2 inhibition on EP1-4 receptors in pups with IVH. IVH was induced by intraperitoneal glycerol at 2 h of age, head ultrasound was performed at 6 h age and then pups were sequentially assigned as (i) glycerol-treated controls without IVH, (ii) celecoxib-treated pups with IVH or (iii) vehicle-treated pups with IVH. Real-time PCR showed that EP1 mRNA accumulation was higher in pups with IVH compared to glycerol-treated controls without IVH at 48 and 72 h postnatal age ($P < 0.05$ each, $n = 5$, Fig. 3A), but not at 12 h of age. However, EP2-4 mRNA expressions were comparable between pups with IVH and glycerol-treated controls without IVH (Fig. 3B–D). Importantly, EP1 expression was significantly suppressed in celecoxib-treated pups with IVH compared to vehicle controls at both 48 and 72 h ($P < 0.05$ each, $n = 5$), but not at 12 h of age (Fig. 3A).

We next asked whether EP1 receptor inhibition would suppress cell death and gliosis in pups with IVH. Thus, we alternatively treated pups with IVH with either subcutaneous SC51089 (10 mg/kg twice daily for 3 days) or vehicle (30 µl sterile water), starting at 6 h of age. The pups were euthanized at 72 h of age and severity of IVH was similar in SC51089- and vehicle-treated controls. TUNEL staining showed lower density of TUNEL positive cells in SC51089-treated pups compared to vehicle controls in the periventricular zone ($P = 0.016$, $n = 5$), but not in the cortex (Fig. 3E). Accordingly, caspase-3/7 activity and neuronal degeneration were significantly reduced in SC51089-treated pups compared to vehicle controls ($P = 0.001$ and 0.013, respectively, $n = 5$) in the periventricular zone, but not in the cerebral cortex (Fig. 3F and G). Furthermore, EP1 receptor inhibition substantially reduced both the astrocyte count in the periventricular region ($P < 0.01$, $n = 5$) and GFAP protein levels (western blot analyses) in the forebrain of pups with IVH compared to controls (Supplementary Fig. 2A and B).

In conclusion, EP1 receptors were elevated in IVH, COX-2 inhibition alleviated EP1 expression, and more importantly, EP1 suppression conferred neuroprotection, just as COX-2 inhibition did.

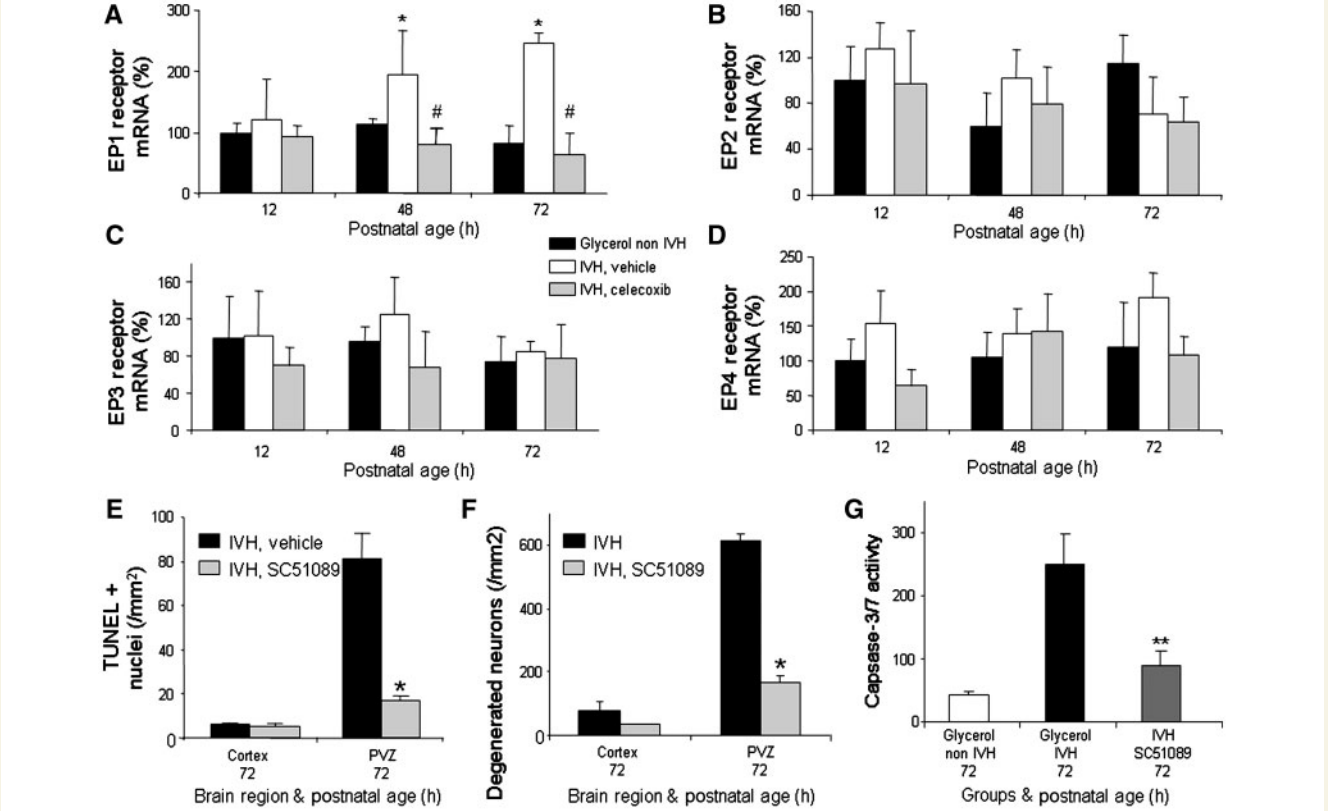

Figure 3 Celecoxib alleviates EP1 in IVH and EP1 inhibition reduces cell death and gliosis. (**A–D**) EP1-4 receptor mRNA expression was assayed by real-time PCR in the forebrain of glycerol controls without IVH, vehicle-treated pups with IVH and celecoxib-treated pups with IVH. Data are mean ± SEM ($n = 5$). EP1 receptor mRNA expression was higher in pups with IVH compared to glycerol-treated controls without IVH at 48 and 72 h postnatal age, but not at 12 h of age. EP1 receptor level was reduced in celecoxib-treated pups compared to vehicle-treated controls. By contrast, EP2-4 receptor levels were comparable between pups with and without IVH. $^{*}P < 0.05$ for pups with IVH (vehicle treated) versus without IVH. $^{\#}P < 0.05$ for celecoxib-treated versus vehicle-treated IVH pups. (**E**) TUNEL positive nuclei were less dense in SC51089-treated pups compared to vehicle-controls in the periventricular zone, but not in the cortex. Data are mean ± SEM ($n = 5$). (**F**) Fluoro Jade B positive neurons were diminished in SC51089-treated pups compared to vehicle controls in the periventricular zone, but not in the cortex. Data are mean ± SEM ($n = 5$). (**G**) Caspase-3/7 activity was significantly reduced in SC51089-treated pups compared to vehicle controls. Data are mean ± SEM ($n = 5$). For **E–G**, $^{*}P < 0.05$ and $^{**}P < 0.01$ for SC51089-treated pups versus vehicle controls. PVZ = periventricular zone.

COX-2 inhibition alleviates consequences of intraventricular haemorrhage—neurological impairment, impaired myelination and gliosis

To determine whether COX-2 inhibition attenuates neurological impairment, we compared motor and sensory evaluation between three sets of premature rabbit pups at Day 14: (i) glycerol treated pups without IVH ($n = 17$); (ii) celecoxib-treated pups with IVH ($n = 16$); and (iii) vehicle-treated pups with IVH ($n = 17$) (Table 1). The severity of IVH in celecoxib-treated pups was comparable to those of vehicle-treated controls with IVH. We noted significant weakness in the foreleg of one and the hind legs of three vehicle-treated IVH pups (23.5%), whereas one pup in the celecoxib-treated group (6%) had weakness in right hind-leg manifesting as asymmetry in gait. The scores for gait were significantly better in celecoxib-treated pups than in vehicle-treated IVH controls ($P = 0.02$). The average distance walked in 60 s was longer in treated pups compared with vehicle controls ($P = 0.027$). The latency to slip down the 60° inclination was substantially longer in the celecoxib-treated pups relative to vehicle controls ($P < 0.001$). The tone in the back legs of three pups with motor impairment in the vehicle-treated group with IVH was slightly increased (score = 1). No difference was observed in sensory and cranial nerve assessment of the three sets of rabbit pups. Importantly, we did not observe any apparent adverse effect attributable to celecoxib treatment among pups with IVH receiving this medication.

We next compared myelination among the three groups of pups at Day 14 ($n = 5$, Fig. 4). Immuno-labelling showed that expression of myelin basic protein was significantly less in vehicle-treated pups with IVH compared to controls without IVH

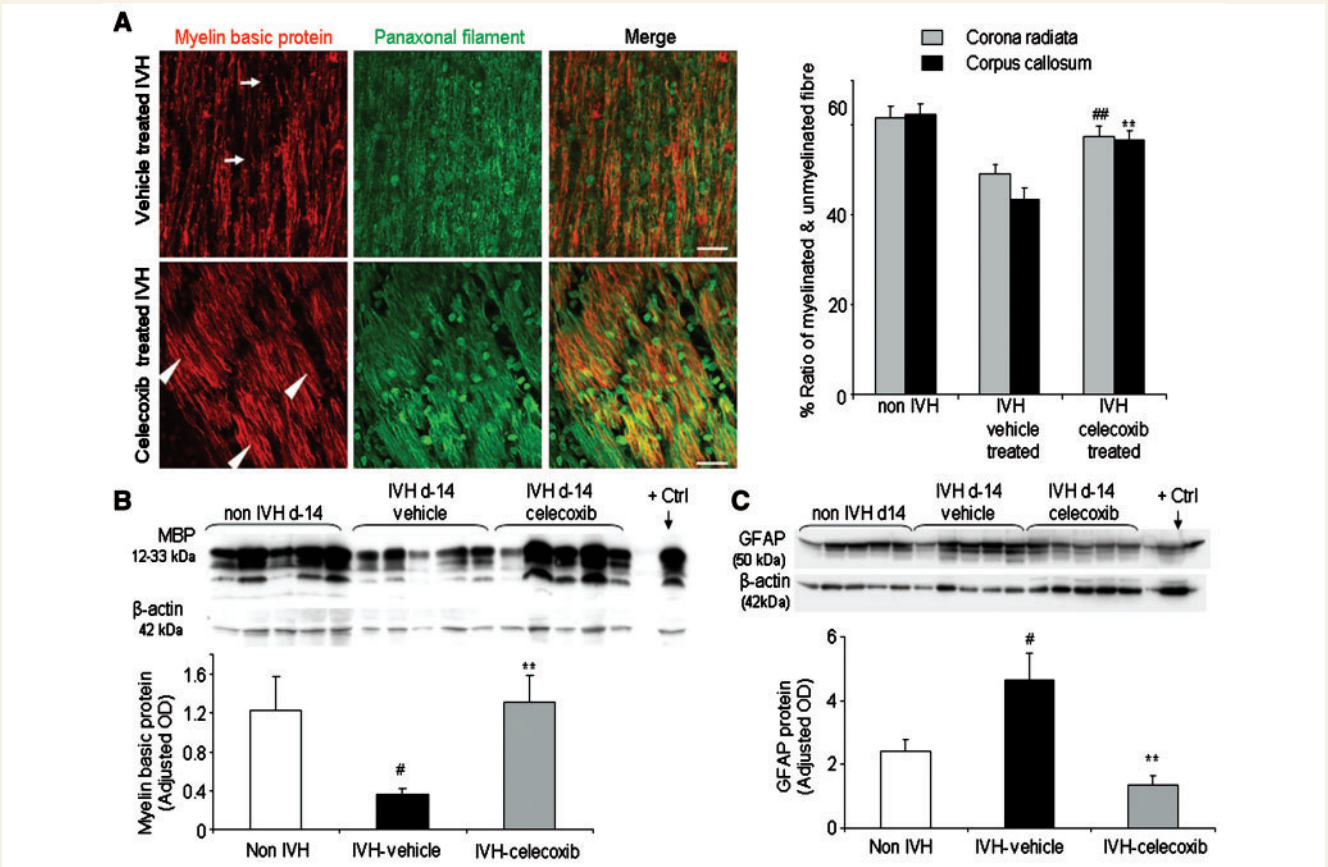

Figure 4 Celexocib treatment restores myelin basic protein and GFAP level in pups with IVH at Day 14. (**A**) Representative immunofluorescence of cryosections stained with myelin basic protein and panaxonal filament antibodies. Note sparse myelinated fibre (arrow) in pups with IVH and dense fibre bundles (arrowhead) in pups without IVH. Data are mean ± SEM ($n = 5$). The ratio of myelinated to unmyelinated fibres was reduced in corona radiata and corpus callosum of pups with IVH when compared to controls without IVH, and celecoxib treatment increased this ratio in pups with IVH. $^{\#\#}P < 0.01$ pups with versus pups without IVH; $^{**}P < 0.01$ celecoxib-treated versus vehicle treated pups with IVH. (**B**) Representative western blot analyses of myelin basic protein in the forebrain of pups without IVH, vehicle-treated pups with IVH and celecoxib-treated pups with IVH at Day 14. Data are mean ± SEM ($n = 5$). Myelin basic protein levels were normalized to β-actin levels. Myelin basic protein levels were less in pups with IVH than in controls without IVH and higher in celecoxib-treated pups than vehicle controls. $^{\#}P < 0.05$ pups with versus those without IVH; $^{**}P < 0.01$ celecoxib-treated versus vehicle-treated pups with IVH. (**C**) Western blot analyses of GFAP in the forebrain of pups without, vehicle-treated pups with and celecoxib-treated pups with IVH at Day 14. Data are mean ± SEM ($n = 5$). GFAP levels were normalized to β actin levels. GFAP levels are greater in pups with when compared to pups without IVH, and lesser in celecoxib-treated pups than in vehicle-treated controls. $^{\#}P < 0.05$ pups with versus those without IVH; $^{**}P < 0.01$ celecoxib-treated versus vehicle-treated pups with IVH. MBP = myelin basic protein; OD = optical density.

in corona radiata and corpus callosum ($P < 0.001$ each), and that celecoxib treatment enhanced the expression of myelin basic protein in these two white matter regions ($P < 0.01$ each, Fig. 4A). Accordingly, western blot analyses revealed that myelin basic protein level was reduced in vehicle-treated pups with IVH when compared to controls without IVH ($P = 0.045$), and celecoxib-treatment enhanced its expression in pups with IVH ($P = 0.01$, Fig. 4B).

We next measured GFAP expression in a) pups without IVH, b) pups with IVH who were treated with celecoxib, and c) vehicle treated pups with IVH at Day 14. Western blot analyses showed that IVH elevated GFAP level ($P = 0.04$, $n = 5$) and celecoxib treatment reduced GFAP expression in pups with IVH at Day 14 ($P = 0.006$, Fig. 4C). In conclusion, celecoxib treatment reduced motor impairment, presumably by enhancing myelination and attenuating gliosis at Day 14.

TNF-α and IL-1β are elevated in intraventricular haemorrhage and COX-2 or EP1 inhibition reduce TNF-α levels, but not IL-1β

Pro-inflammatory cytokines TNF-α and IL-1β are increased in adult animal model of brain haemorrhage, contributing to the brain damage (Mayne *et al*., 2001); and COX-2 inhibition suppresses TNF-α production in neuronal culture experiments (Araki *et al*., 2001). It was, therefore important to determine whether TNF-α

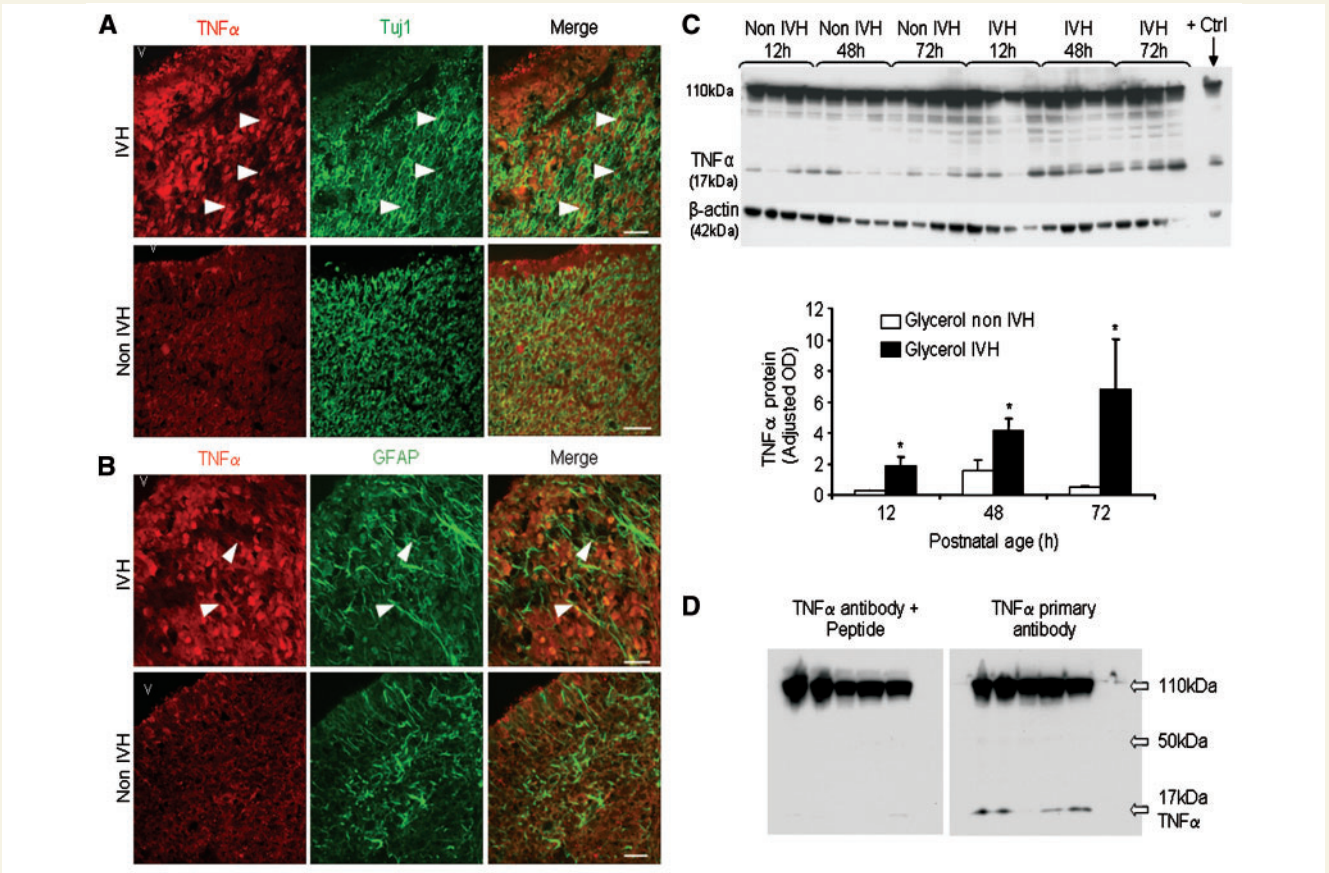

Figure 5 Higher TNF-α in pups with IVH than in those without IVH. (**A**) Representative immunofluorescence of cryosections from the germinal matrix of 72 h premature pup double labelled with TNF-α and Tuj1-specific antibody. Expression of TNF-α was higher in pups with IVH than controls without IVH. TNF-α positive immunoreactivities partly co-localized with Tuj1 positive signals (arrowhead). V = ventricle. Scale bar, 20 μm. (**B**) Cryosections were double-stained with TNF-α and GFAP-specific antibody. TNF-α was expressed on some of the GFAP positive astrocytes (arrowhead). Inset in the merge image show partial overlap of TNF-α positive immunoreactivities on the GFAP (+) astrocytes. Scale bar = 20 μm. (**C**) Representative western blot analysis for TNF-α in the forebrain of premature rabbit pups with and without IVH. Data are mean ± SEM ($n = 4$ at each time point). Data normalized to β-actin. The blot shows two major bands: 17 and 110 kDa. TNF-α (17 kDa) concentration was greater in pups with IVH than in controls without IVH at each epoch. *$P < 0.05$ for pups with versus those without IVH. (**D**) Peptide competition to demonstrate specificity of 17-kDa TNF-α band. Lysates from brain of five pups with IVH were loaded into well #1–5 of 4–20% gradient precast gel (Biorad, CA, USA) and then the same brain-lysates were loaded into well #11–15 of the same gel. Other wells on the gel were empty. The separated proteins were transferred to polyvinylidene difluoride membrane by electrotransfer. The membrane was divided into two so that each piece of the membrane had five lanes containing protein form IVH brains. One piece of the membrane was incubated with primary antibody and other with antibody pre-absorbed with peptide (based on manufacturer's protocol). Target proteins were detected with enhanced chemiluminescence system (Amersham), using secondary antibodies. The membrane incubated with primary antibody depicted bands at 17 and 110 kDa, whereas membrane incubated with antibody pre-absorbed with peptide showed only 110 kDa band. This suggested that 17 kDa band was specific to TNF-α.

and IL-1β were elevated in pups with IVH and if COX-2 or EP1 inhibition reduced TNF-α and IL-1β levels. To this end, we evaluated protein expression of TNF-α in pups both with and without IVH using immunohistochemistry and western blot analyses. TNF-α was abundant in the periventricular zone of pups with IVH, but sparse in controls without IVH (Fig. 5A and B). TNF-α was weakly expressed in the cerebral cortex of both pups with and without IVH. Double immunolabelling of brain section with TNF-α combined with Tuj1 or GFAP confirmed that TNF-α was expressed in several immature neurons and also in some of the astrocytes of the periventricular zone in pups with IVH (Fig. 5A and B). Furthermore, TNF-α was also weakly expressed in microglia labelled with tomato lectin (data not shown). Western blot analyses show two sets of bands: 17 and 110 kDa. The 17 kDa band matches with the molecular weight of TNF-α (Fig. 5C and D). To determine the specificity of these bands we performed peptide competition. Briefly, we incubated in polyvinylidene difluoride membrane after protein transfer into primary antibody or primary antibody pre-absorbed with peptide (specific to TNF-α antibody). The membrane incubated with primary antibody depicted bands at 17 and 110 kDa, whereas membrane incubated with antibody pre-absorbed with peptide showed only the 110 kDa band

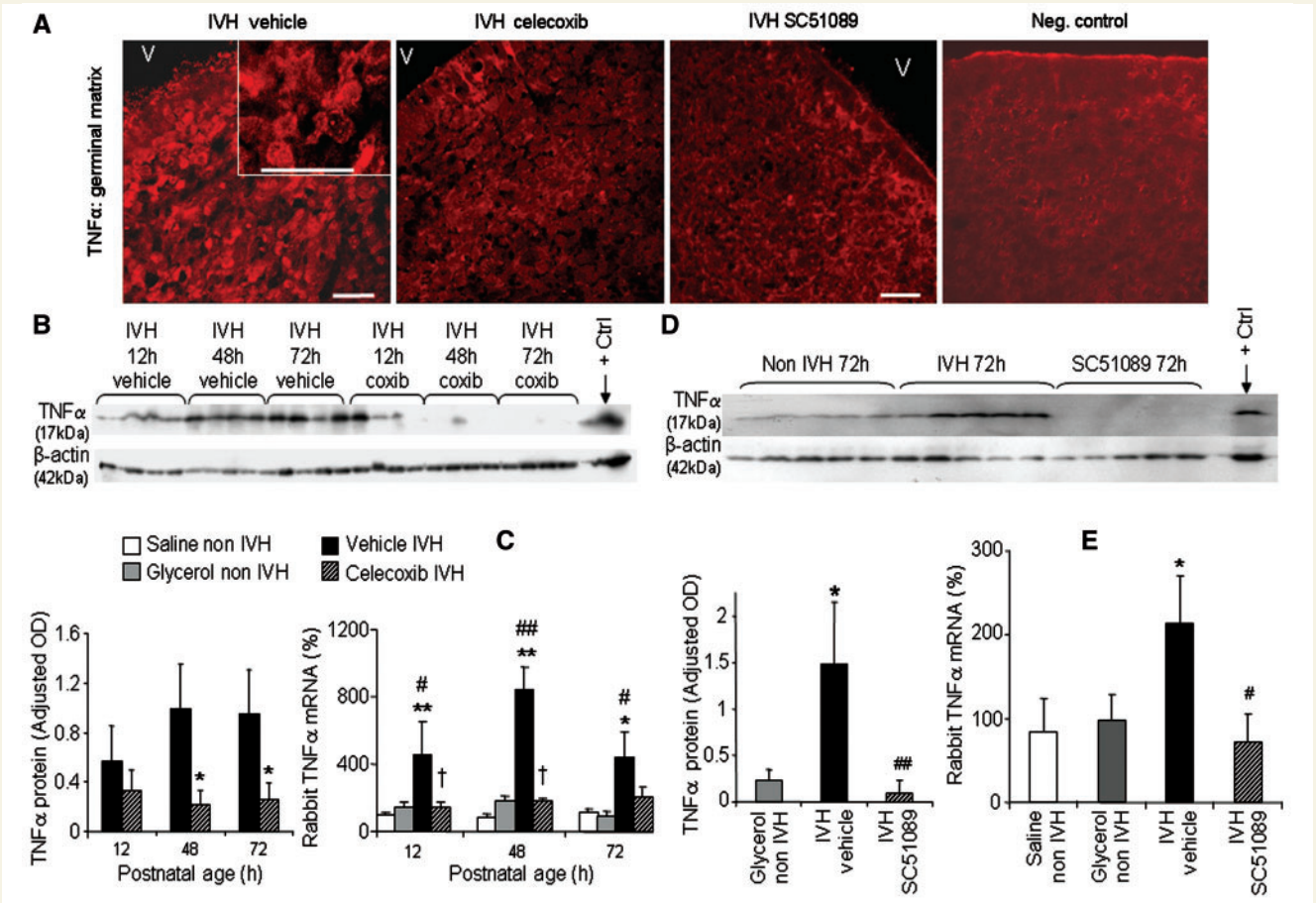

Figure 6 High TNF-α occurs in IVH, and celecoxib or SC51089 suppresses TNF-α expression. (**A**) Representative immunofluorescence of cryosections from germinal matrix of 72 h old premature pup labelled with TNF-α-specific antibody. TNF-α was abundantly expressed in the germinal matrix of vehicle-treated pups with IVH, but weakly in celecoxib- or SC10589-treated pups. Inset shows TNF-α expression in the neural cells of the germinal matrix under high magnification. Negative control (indicated) was made by incubating IVH brain section with TNF-α antibody pre-absorbed with its blocking peptides. Note a relative absence of immunoreactivity in this control section. Scale bar, 20 μm. V = ventricle. (**B**) Representative western blot analysis of TNF-α in forebrain of celecoxib- and vehicle- (control) treated pups with IVH. Human breast carcinoma tissue lysate was the positive control. Data are mean ± SEM ($n = 8$ each time point). Values were normalized to β-actin. TNF-α protein levels were significantly lower in celecoxib-treated pups with IVH compared to vehicle-treated controls with IVH at 48 and 72 h, but not at 12 h postnatal age. $^{*}P < 0.05$ for celecoxib- versus vehicle-treated pups with IVH. (**C**) TNF-α mRNA expression was assayed by real time PCR. Data are mean ± SEM ($n = 6$ for each time point). TNF-α gene expression was substantially higher in pups with IVH compared to saline- and glycerol-treated controls without IVH at 12, 48 and 72 h of age, and celecoxib treatment reduced TNF-α mRNA expression in pups with IVH at 12 and 48 h, but not at 72 h of age. $^{*}P < 0.05$, $^{**}P < 0.01$ saline-treated pups without IVH versus vehicle treated pups with IVH; $^{\#}P < 0.05$, $^{\#\#}P < 0.01$ glycerol-treated pups without IVH versus vehicle treated pups with IVH; $^{\dagger}P < 0.05$ celecoxib- versus vehicle-treated pups with IVH. (**D**) Representative western blot analysis of TNF-α in forebrain of pups without, vehicle-treated pups with and SC51089-treated pups with IVH at 72 h of age. Data are mean ± SEM ($n = 5$). Values were normalized to β-actin. TNF-α protein levels were significantly greater in pups with IVH than controls without IVH, and SC51089 attenuated TNF-α levels in pups with IVH. $^{*}P < 0.05$ for pups without versus those with IVH; $^{\#\#}P < 0.01$ for SC51089- versus vehicle-treated pups with IVH. (**E**) TNF-α mRNA expression was assayed by real time PCR. Data are mean ± SEM ($n = 6$). TNF-α gene expression was significantly higher in pups with IVH compared to saline-treated and glycerol-treated controls without IVH and SC51089 reduced TNF-α gene expression. $^{*}P < 0.05$ for pups without versus those with IVH; $^{\#}P < 0.05$ for SC51089- versus vehicle-treated pups with IVH.

(Fig. 5D). This suggested that the 17 kDa band was specific to TNF-α. TNF-α levels (17 kDa) were significantly greater in pups with IVH compared to controls at 12, 48 and 72 h of age ($P = 0.03$, 0.05 and 0.02).

We compared TNF-α levels between celecoxib-treated pups with IVH and vehicle-treated controls without IVH. Immunolabelling showed that TNF-α expression in the periventricular zone was diminished in celecoxib-treated pups compared to vehicle-treated controls (Fig. 6A). Western blot analyses confirmed that TNF-α protein levels were markedly reduced in celecoxib-treated pups with IVH compared to vehicle-treated controls at 48 and 72 h ($P < 0.03$ and 0.02, $n = 8$ at each epoch,

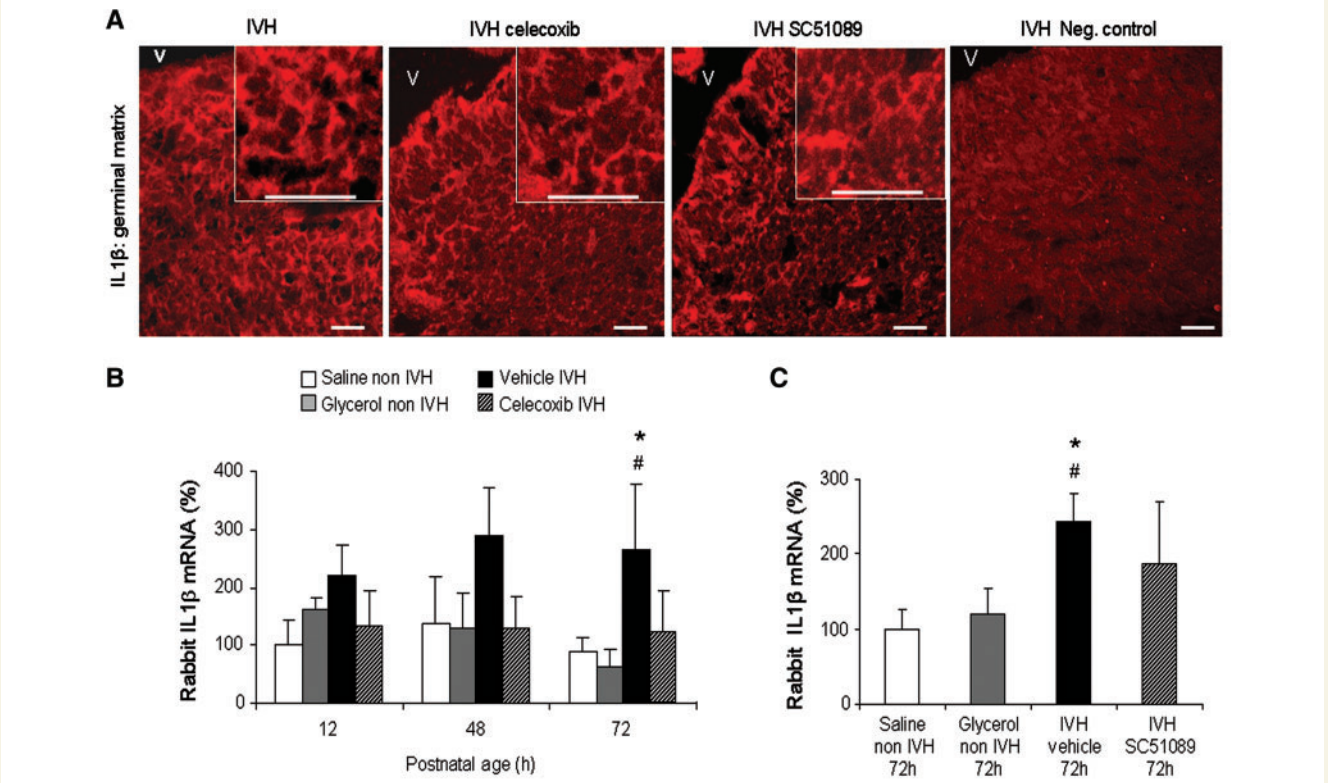

Figure 7 Elevated IL-1β in pups with IVH, and celecoxib or SC51089 does not affect IL-1β expression. (**A**) Representative immunofluorescence of cryosections from germinal matrix of 72 h old premature pups labelled with IL-1β specific antibody. IL-1β was abundantly expressed in the germinal matrix of vehicle-treated pups with IVH, and IL-1β expression was similar in vehicle-, celecoxib- or SC10589-treated pups with IVH. Inset shows IL-1β expression in the neural cells of the germinal matrix under high magnification. Negative control (shown) was made by incubating IVH brain section with IL-1β antibody pre-absorbed with its blocking peptides. Note a relative absence of immunoreactivity in this control section. Scale bar, 20 μm. V = ventricle. (**B**) IL-1β mRNA level was measured by real-time quantitative PCR. Data are mean ± SEM ($n = 6$ each group). IL-1β mRNA expression was higher in pups with IVH compared to saline- or glycerol-treated pups without IVH at 72 h age of age, but not at 24 and 48 h of age. Celecoxib treatment did not significantly affect IL-1β gene levels. (**C**) IL-1β gene expression was assayed by real time PCR. Data are mean ± SEM ($n = 6$ for each group). IL-1β gene expression was higher in pups with IVH compared to saline- and glycerol-treated controls without IVH at 72 h postnatal age. SC51089 did not substantially affect IL-1β gene expression. $^{*}P < 0.05$ for saline-treated pups without versus those with IVH; $^{\#}P < 0.05$ for glycerol-treated pups without versus those with IVH.

Fig. 6B), but not at 12 h of age ($P = 0.07$, $n = 8$ each). Accordingly, real-time PCR showed that TNF-α mRNA accumulation was significantly higher in pups with IVH compared to saline- and glycerol-treated controls without IVH at 12, 48 and 72 h ($P < 0.05$ each, $n = 6$ each, Fig. 6C). In addition, celecoxib treatment significantly reduced TNF-α mRNA expression in pups with IVH at 12 and 48 h ($P < 0.045$, 0.03, $n = 6$ each), but not at 72 h of age ($P = 0.1$, $n = 6$ each). We then evaluated the effect of SC51089, an EP1 blocker, on TNF-α expression in pups with IVH compared to vehicle controls at 72 h of age. Immunohistochemistry showed that TNF-α immuoreactivity in the periventricular region was less in SC51089-treated pups when compared to vehicle-treated controls with IVH (Fig. 6A). Accordingly, TNF-α protein, measured by western blot analyses, was almost undetectable in the treatment group at 72 h of age ($P < 0.01$, Fig. 6D). Similarly, real time PCR revealed that TNF-α expression was significantly reduced in pups with IVH upon SC51089 treatment at 72 h of age ($P < 0.04$, $n = 6$ each, Fig. 6E).

We next evaluated IL-1β levels in the same paradigm as TNF-α expression. Immunohistochemistry showed that IL-1β was strongly expressed in the periventricular zone of pups with IVH and weakly in controls without IVH (Supplementary Fig. 4). Double immunolabelling confirmed that IL-1β was expressed in the immature neurons and some of the astrocytes in the periventricular zone of pups with IVH. IL-1β immunoreactivity was weak in the cerebral cortex of pups with and without IVH. Consistent with protein expression, IL-1β mRNA expression was higher in pups with IVH compared to controls without IVH at 72 h of age, but not at 12 and 48 h of age ($n = 6$ each, Fig. 7B). Importantly, both IL-1β immunoreactivity and mRNA expression were also comparable in vehicle-, celecoxib- and SC51089-treated IVH pups at 72 h of age (Fig. 7A–C). In conclusion, IVH upregulates TNF-α and IL-1β

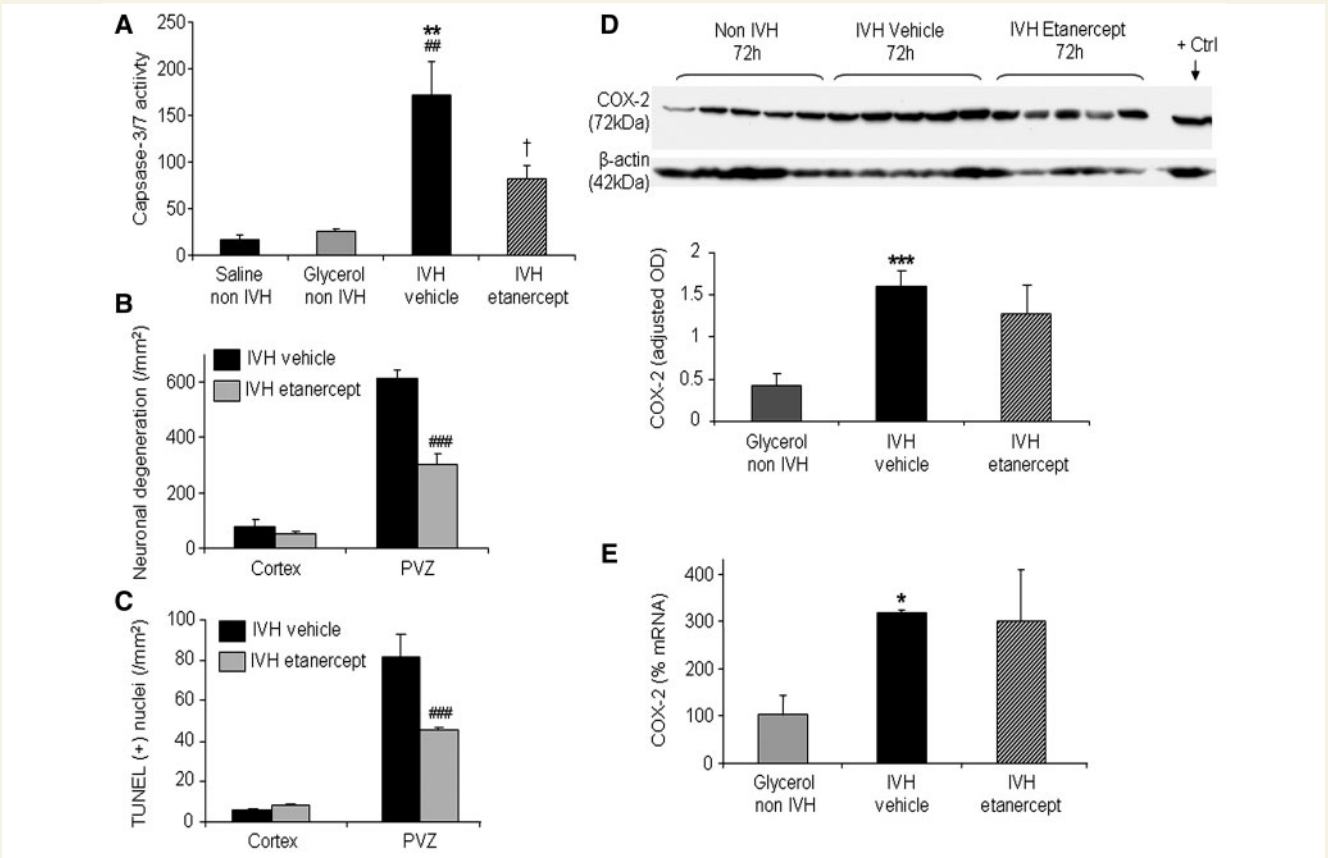

Figure 8 TNF-α inhibition does not affect COX-2 level, but reduces caspase-3/7 and cell death. (**A**) Caspase-3/7 activity was measured in the forebrain brain homogenate of pups with IVH treated with etanercept, those treated with vehicle and pups without IVH. Data are mean ± SEM ($n = 6$). Caspase-3/7 activity was significantly greater in pups with IVH compared to controls without IVH and etanercept significantly reduced caspase-3/7 activity. $^{**}P < 0.01$ saline-treated pups without IVH versus vehicle-treated pups with IVH, $^{\#\#}P < 0.01$ glycerol-treated pups without IVH versus vehicle-treated pups with IVH, $^{\dagger}P < 0.05$ etanercept-treated pups with IVH versus vehicle controls. (**B**) Neuronal degeneration was assessed by Fluor-JadeB staining. Data are mean ± SEM ($n = 6$). Neuronal degeneration was significantly less in IVH pups treated with etanercept compared to vehicle controls in the periventricular zone of the brain, but not in the cortex. $^{\#\#\#}P < 0.001$ for etanercept-treated pups with IVH versus vehicle controls. (**C**) TUNEL staining was evaluated in etanercept-treated and vehicle-treated pups with IVH. Data are mean ± SEM ($n = 6$). TUNEL positive nuclei were less dense in etanercept-treated than vehicle-treated pups. $^{\#\#\#}P < 0.001$ for etanercept-treated pups with IVH versus vehicle controls. (**D**) Representative western blot analyses of COX-2 in the forebrain of pups without, vehicle-treated pups with, and etanercept-treated pups with IVH at 72 h of age. Data are mean ± SEM ($n = 5$ each). Values were normalized to β-actin. COX-2 protein level was greater in pups with IVH than in controls without IVH and etanercept did not affect COX-2 levels. $^{***}P < 0.001$ for vehicle treated pups with IVH versus glycerol-treated controls without IVH. (**E**) COX-2 mRNA level, assayed by real time quantitative PCR was higher in pups with IVH than in controls without IVH and etanercept did not influence COX-2 levels. Data are mean ± SEM ($n = 6$). $^{*}P < 0.05$ for pups with IVH versus without IVH.

expression; and celecoxib or SC51089 alleviates TNF-α, but not IL-1β levels in pups with IVH.

Etanercept reduces cell death and gliosis, and does not affect COX-2 expression

As both COX-2 and EP1 inhibition distinctly attenuated TNF-α expression in our experiment, and since TNF-α mediates inflammatory brain damage (Crisafulli *et al.*, 2009), it was crucial to determine whether TNF-α inhibition offers neuroprotection in pups with IVH. We used etanercept as a TNF-α antagonist. It is a dimeric fusion protein that binds specifically to TNF-α and blocks its interaction with cell surface TNF receptors. We treated pups with IVH with either intra-cereboventricular etanercept (2 mg/kg diluted to 20 μl—one dose in each lateral ventricle) or vehicle at 6 h of age. The pups were euthanized at 72 h of age and severity of IVH was similar in etanercept- and vehicle-treated controls. We found that caspase-3/7 levels were significantly reduced in treated pups compared to vehicle controls ($P < 0.05$, $n = 6$ each, Fig. 8A). We next assessed apoptotic cell death and neuronal degeneration in treated and control pups. Both TUNEL positive nuclei and

Fluoro Jade B positive neurons were substantially less in etanercept-treated pups compared to vehicle controls in the periventricular zone ($P < 0.001$ each, $n = 6$ each), but not in the cortex (Fig. 8B and C). Finally, the number of astrocytes was significantly reduced in etanercept-treated pups compared to vehicle controls in the periventricular zone ($P < 0.01$ each, $n = 6$ each), but not in the cortex (Supplementary Fig. 2A). GFAP content, measured by western blot analysis, was also substantially reduced in the etanercept-treated pups compared to controls (Supplementary Fig. 2B).

As pharmacological inhibition of TNF-α suppresses COX-2 levels in a culture model of peritoneal macrophages (Crisafulli *et al*., 2009), it was important to assess whether TNF-α inhibition reduced COX-2 levels in our animal model. Western blot analysis revealed that COX-2 protein expression in etanercept-treated pups with IVH and vehicle-treated controls were comparable (Fig. 8D). Consistent with protein measurement, COX-2 gene expression was similar between etanercept-treated IVH pups and vehicle controls ($n = 6$ each, Fig. 8E). In conclusion, TNF inhibition with etanercept suppressed cell death and gliosis, but not COX-2 levels.

Discussion

As both birth rate and survival of premature neonates have increased over the last few decades, IVH and its attendant complications—cerebral palsy and cognitive deficits—have developed as major public health concerns (Shennan and Bewley, 2006; Stephens and Vohr, 2009). No therapeutic strategy exists to curtail the devastating cascades of pathological events triggered in the haemorrhaging brain of premature infants. The present study highlights a unique set of mechanistically linked molecules—COX-2, EP1 and TNF-α—whose levels were elevated in pups with IVH compared to controls without IVH; and more importantly, that inhibition of any of the three prevented cell infiltration, neural cell death and gliosis during the first 3 days of life. We found that COX-2 inhibition by celecoxib treatment restored neurological impairment, enhanced myelination and reduced gliosis at Day 14. Furthermore, our study revealed novel molecular links indicating that EP1 and TNF-α were downstream of COX-2 in the inflammatory cascade triggered by IVH.

The most important and novel observation in this study was the identification of a set of mechanistically interwoven molecules: COX-2, EP1 and TNF-α, which were upregulated in IVH. Importantly, each of the three molecules offered short-term neuroprotection on separate preclinical testing. Moreover, neurobehavioural assessment at Day 14 showed that celecoxib-treated (7-day regimen) pups display superior motor function and greater myelination compared to vehicle-treated controls. Consistent with our findings, COX-2 is markedly upregulated in ischaemic, degenerative and traumatic brain injuries and mediates tissue damage (Gopez *et al*., 2005; Candelario-Jalil and Fiebich, 2008). COX-2 activation exerts neurotoxicity primarily by (i) inducing oxidative stress; (ii) contributing to glutamate excitotoxicity; and (iii) promoting cell-cycle activity (Candelario-Jalil and Fiebich, 2008). Indeed, COX-2 inhibition by celecoxib treatment induces neurological recovery in adult animals after intracerebral haemorrhage (Chu *et al*., 2004). In addition, selective COX-2 inhibition alleviates motor impairment in the G93A superoxide dismutase mouse model of amyotrophic lateral sclerosis (Pompl *et al*., 2003), and celecoxib is undergoing clinical trials to mitigate neuroinflammation in amyotrophic lateral sclerosis (Gordon *et al*., 2008). Hence, COX-2 inhibition could be a viable strategy of neuroprotection for IVH in premature infants.

PGE2 exerts neurologically adverse effects via prostaglandin receptor subtype EP1 (Bilak *et al*., 2004; Manabe *et al*., 2004). EP1 activation disrupts calcium homeostasis, contributing to excitotoxic neuronal-degeneration in an adult rat model of hypoxia-ischaemia (Kawano *et al*., 2006). In addition, pharmacological inhibition or gene inactivation of EP1 alleviates brain damage produced by focal cerebral ischaemia, excitotoxicity and glucose deprivation (Ahmad *et al*., 2006; Kawano *et al*., 2006). Consistent with these reports, we observed that EP1 blockage by subcutaneous SC51089 treatment reduced apoptosis, neuronal degeneration and gliosis in pups with IVH. Of note, COX-2 inhibition with celecoxib exacerbates the risk of cardiovascular thrombotic events, myocardial infarction and stroke in adults. In addition, COX-2 inhibition might impair renal function in neonates (Prevot *et al*., 2004). Therefore, EP1—a downstream effector of COX-2—inhibition might offer a safer and superior therapeutic strategy for neuroprotection in premature infants with IVH compared to COX-2 inhibition.

We demonstrated the neuroprotective ability of TNF-α inhibition in our model of IVH. TNF-α signalling is involved in every facet of inflammatory brain injury and results in two major responses: apoptosis and inflammation (Hallenbeck, 2002). It has a large signalling network, which initiates activation of caspases (apoptosis), matrix metalloproteinases, xanthine oxidase, nicotinamide adenine dinucleotide phosphate oxidase and inducible nitric oxide synthase (generation of free radicals), and potentiates *N*-methyl-D-aspartate receptor-mediated neurotoxicity (Hallenbeck, 2002; Hosomi *et al*., 2005; Hua *et al*., 2006). Both TNF-α knockout mice and antisense oligodeoxynucleotide-treated adult rats with brain haemorrhage exhibit diminished cell death and inflammation compared to controls (Mayne *et al*., 2001; Hua *et al*., 2006). Indeed, anti-TNF-α therapy is in extensive clinical use for inflammatory disorders including rheumatoid arthritis, psoriasis and other conditions (Palladino *et al*., 2003). Similar, and in agreement to these observations, we found that etanercept, a TNF-α inhibitor, attenuated cell death and inflammation. Hence, TNF-α inhibition could be another important strategy to abrogate brain injury in premature infants with IVH.

Our experiments revealed a novel mechanistic connection between TNF-α, COX-2 and EP1. Specifically, COX-2 and EP1 suppression reduced TNF-α levels, while TNF-α inhibition did not influence COX-2 expression. In agreement to our findings, it has been reported that COX-2 inhibition by NS-398 reduces TNF-α elevation and neuronal cell death in neuronal culture experiments (Araki *et al*., 2001). However, in contrast to our results, both genetic and pharmacological inhibition of TNF-α significantly reduces COX-2 expression in peritoneal macrophages in culture experiment; and TNF-α triggers upregulation of COX-2 expression in HT-29 cells (Ikawa *et al*., 2001; Crisafulli *et al*., 2009). We

could not find any *in vivo* experiments in brain showing that TNF-α directly regulates COX-2. Therefore, it is plausible that COX-2 and EP1 are upstream molecules that regulate TNF-α expression in premature infants with brain injuries. Our previous work has shown that Tuj1 positive immature neurons constitute the predominant population of degenerating and dying cells around the ventricle of the haemorrhaging brain (Georgiadis *et al*., 2008). Accordingly, the present study revealed an abundance of COX-2 and TNF-α in the Tuj1 positive neurons in the periventricular zone, and suppression of either COX-2 or TNF-α reduced neuronal cell death in this brain region. A study, which is also consistent with our findings, has shown that intracerebral injection TNF-α in neonatal rat (P5) results in astrogliosis and neuronal cell death (Cai *et al*., 2004). In another study performed on APP/PS1 mice, inhibition of nuclear factor-κB—a downstream mediator of TNF-α—has attenuated gliosis (Zhang *et al*., 2009). Indeed, TNF-α is a mediator of cell death and gliosis both *in vitro* and *in vivo* (Hallenbeck, 2002; Hosomi *et al*., 2005; Hua *et al*., 2006). Taking these facts together, COX-2 seems to be an upstream molecule in a neonatal model of brain injuries that induces cell death and gliosis via upregulating TNF-α and not the reverse.

IVH results in cerebral palsy and cognitive deficits in premature infants. At this time, there is no treatment of IVH and active withdrawal of life support from premature infants with severe IVH based on quality of life concerns, although infrequent, does occur (Sawyer, 2008). Our study showed clinical recovery in treated pups compared to untreated controls. Furthermore, we did not observe any apparent adverse effects attributable to celecoxib in pups with IVH receiving this medication. Unfortunately, neither celecoxib nor the other two treatments—EP1 and TNF inhibitor—are approved by the Food and Drug Administration for use in newborns. Nevertheless, celecoxib has a broad experience in human application and therefore, testing its utility in a phase I-type clinical trial in human neonates with severe IVH (grade III or IV, Papile Scale) appears to have merit.

Of note, neurological outcome of IVH is principally determined by the severity of haemorrhage and extent of parenchymal involvement (Brouwer *et al*., 2008). Similarly in our model, we observed three grades of IVH, including microscopic (mild), gross blood in the ventricle (moderate) or large haemorrhage resulting in fusion of the two lateral ventricles (severe). In our previous study, we observed abundant inflammatory cells (neutrophil and microglial), apoptosis and neuronal degeneration in the periventricular region at 24, 48 and 72 h of age in pups with IVH, whereas these inflammatory changes were not significantly present in glycerol-treated or in saline-treated controls without IVH (Georgiadis *et al*., 2008). Furthermore, cellular infiltration and death are minimal in microscopic IVH in contrast to pups with moderate-to-severe IVH. Therefore, in the present study, we included only pups with moderate-to-severe IVH to evaluate the effect of the three neuroprotectants. We also ascertained that the comparison groups are balanced with respect to the severity of IVH. However, the present study did not assess COX-2, EP-1 and cytokine levels as a function of severity of IVH—moderate versus severe haemorrhage.

In conclusion, we demonstrated that COX-2, EP1 or TNF-α inhibition attenuated inflammation, cell death and gliosis induced by IVH in premature rabbit pups, and that COX-2 inhibition by celecoxib treatment also promotes long term recovery in motor function and myelination. The three molecules—COX-2, EP1 and TNF-α—are mechanistically linked in a signalling cascade with COX-2 and EP1 upstream to TNF-α. The suppression of any of the three might minimize the brain injury in premature infants with IVH. If translated into human investigation, the results of this study might positively impact the survival and neurological outcome of premature infants with IVH. These data provide a fundamental and mechanistic rationale to conduct a phase I-type therapeutic trial.

Acknowledgements

The authors thank Dr Victor Fried, PhD for his advice on cytokine assay in our materials. The authors thank Dr Carl Thompson, PhD for statistical advice.

Funding

Pfizer Inc. (PB); American Heart Association Grant-in-Aid (PB); National Institute of Health/National Institute of Neurological Disorders and Stroke NS0505586 (PB).

Supplementary material

Supplementary material is available at *Brain* online.

References

Ahmad AS, Ahmad M, de Brum-Fernandes AJ, Dore S. Prostaglandin EP4 receptor agonist protects against acute neurotoxicity. Brain Res 2005; 1066: 71–7.

Ahmad AS, Saleem S, Ahmad M, Dore S. Prostaglandin EP1 receptor contributes to excitotoxicity and focal ischemic brain damage. Toxicol Sci 2006; 89: 265–70.

Ahmad M, Zhang Y, Liu H, Rose M, Graham SH. Prolonged opportunity for neuroprotection in experimental stroke with selective blockade of cyclooxygenase-2 activity. Brain Res 2009.

Alvarez-Soria MA, Largo R, Sanchez-Pernaute O, Calvo E, Egido J, Herrero-Beaumont G. Prostaglandin E2 receptors EP1 and EP4 are up-regulated in rabbit chondrocytes by IL-1beta, but not by TNFalpha. Rheumatol Int 2007; 27: 911–7.

Araki E, Forster C, Dubinsky JM, Ross ME, Iadecola C. Cyclooxygenase-2 inhibitor ns-398 protects neuronal cultures from lipopolysaccharide-induced neurotoxicity. Stroke 2001; 32: 2370–5.

Ballabh P, Xu H, Hu F, Braun A, Smith K, Rivera A, et al. Angiogenic inhibition reduces germinal matrix hemorrhage. Nat Med 2007; 13: 477–85.

Bilak M, Wu L, Wang Q, Haughey N, Conant K, St Hillaire C, et al. PGE2 receptors rescue motor neurons in a model of amyotrophic lateral sclerosis. Ann Neurol 2004; 56: 240–8.

Brambilla R, Burnstock G, Bonazzi A, Ceruti S, Cattabeni F, Abbracchio MP. Cyclo-oxygenase-2 mediates P2Y receptor-induced reactive astrogliosis. Br J Pharmacol 1999; 126: 563–7.

Braun A, Xu H, Hu F, Kocherlakota P, Siegel D, Chander P, et al. Paucity of pericytes in germinal matrix vasculature of premature infants. J Neurosci 2007; 27: 12012–24.

Broughton BR, Reutens DC, Sobey CG. Apoptotic mechanisms after cerebral ischemia. Stroke 2009; 40: e331–9.

Brouwer A, Groenendaal F, van Haastert IL, Rademaker K, Hanlo P, de Vries L. Neurodevelopmental outcome of preterm infants with severe intraventricular hemorrhage and therapy for post-hemorrhagic ventricular dilatation. J Pediatr 2008; 152: 648–54.

Cai Z, Lin S, Pang Y, Rhodes PG. Brain injury induced by intracerebral injection of interleukin-1beta and tumor necrosis factor-alpha in the neonatal rat. Pediatr Res 2004; 56: 377–84.

Candelario-Jalil E, Fiebich BL. Cyclooxygenase inhibition in ischemic brain injury. Curr Pharm Des 2008; 14: 1401–18.

Chu K, Jeong SW, Jung KH, Han SY, Lee ST, Kim M, et al. Celecoxib induces functional recovery after intracerebral hemorrhage with reduction of brain edema and perihematomal cell death. J Cereb Blood Flow Metab 2004; 24: 926–33.

Chua CO, Chahboune H, Braun A, Dummula K, Chua CE, Yu J, et al. Consequences of intraventricular hemorrhage in a rabbit pup model. Stroke 2009; 40: 3369–77.

Cimino PJ, Keene CD, Breyer RM, Montine KS, Montine TJ. Therapeutic targets in prostaglandin E2 signaling for neurologic disease. Curr Med Chem 2008; 15: 1863–9.

Crisafulli C, Galuppo M, Cuzzocrea S. Effects of genetic and pharmacological inhibition of TNF-alpha in the regulation of inflammation in macrophages. Pharmacol Res 2009; 60: 332–40.

Derrick M, Luo NL, Bregman JC, Jilling T, Ji X, Fisher K, et al. Preterm fetal hypoxia-ischemia causes hypertonia and motor deficits in the neonatal rabbit: a model for human cerebral palsy? J Neurosci 2004; 24: 24–34.

FitzGerald GA. COX-2 and beyond: approaches to prostaglandin inhibition in human disease. Nat Rev Drug Discov 2003; 2: 879–90.

Georgiadis P XH, Chua C, Hu F, Collins L, Huynh C, LaGamma EF, et al. Characterization of acute brain injuries and neurobehavioral profiles in a rabbit model of germinal matrix hemorrhage. Stroke 2008; 39: 3378–88.

Gopez JJ, Yue H, Vasudevan R, Malik AS, Fogelsanger LN, Lewis S, et al. Cyclooxygenase-2-specific inhibitor improves functional outcomes, provides neuroprotection, and reduces inflammation in a rat model of traumatic brain injury. Neurosurgery 2005; 56: 590–604.

Gordon PH, Cheung YK, Levin B, Andrews H, Doorish C, Macarthur RB, et al. A novel, efficient, randomized selection trial comparing combinations of drug therapy for ALS. Amyotroph Lateral Scler 2008; 9: 212–22.

Hallenbeck JM. The many faces of tumor necrosis factor in stroke. Nat Med 2002; 8: 1363–8.

Heuchan AM, Evans N, Henderson Smart DJ, Simpson JM. Perinatal risk factors for major IVH in the Australian and New Zealand Neonatal Network, 1995-97. Arch Dis Child Fetal Neonatal Ed 2002; 86: F86–90.

Hosomi N, Ban CR, Naya T, Takahashi T, Guo P, Song XY, et al. Tumor necrosis factor-alpha neutralization reduced cerebral edema through inhibition of matrix metalloproteinase production after transient focal cerebral ischemia. J Cereb Blood Flow Metab 2005; 25: 959–67.

Hua Y, Wu J, Keep RF, Nakamura T, Hoff JT, Xi G. Tumor necrosis factor-alpha increases in the brain after intracerebral hemorrhage and thrombin stimulation. Neurosurgery 2006; 58: 542–50; discussion 542–50.

Hwang SY, Jung JS, Kim TH, Lim SJ, Oh ES, Kim JY, et al. Ionizing radiation induces astrocyte gliosis through microglia activation. Neurobiol Dis 2006; 21: 457–67.

Investigators of the Vermont-Oxford Trial Network Database Project. The Vermont-Oxford Trials Network: very low birth weight outcomes for 1990. Pediatrics 1993; 91: 540–5.

Ikawa H, Kameda H, Kamitani H, Baek SJ, Nixon JB, Hsi LC, et al. Effect of PPAR activators on cytokine-stimulated cyclooxygenase-2 expression in human colorectal carcinoma cells. Exp Cell Res 2001; 267: 73–80.

Kaur C, Ling EA. Periventricular white matter damage in the hypoxic neonatal brain: Role of microglial cells. Prog Neurobiol 2009; 87: 264–80.

Kawano T, Anrather J, Zhou P, Park L, Wang G, Frys KA, et al. Prostaglandin E2 EP1 receptors: downstream effectors of COX-2 neurotoxicity. Nat Med 2006; 12: 225–9.

Laemmli UK, Beguin F, Gujer-Kellenberger G. A factor preventing the major head protein of bacteriophage T4 from random aggregation. J Mol Biol 1970; 47: 69–85.

Manabe Y, Anrather J, Kawano T, Niwa K, Zhou P, Ross ME, et al. Prostanoids, not reactive oxygen species, mediate COX-2-dependent neurotoxicity. Ann Neurol 2004; 55: 668–75.

Martinet L, Fleury-Cappellesso S, Gadelorge M, Dietrich G, Bourin P, Fournie JJ, et al. A regulatory cross-talk between Vgamma9Vdelta2 T lymphocytes and mesenchymal stem cells. Eur J Immunol 2009; 39: 752–62.

Mayne M, Ni W, Yan HJ, Xue M, Johnston JB, Del Bigio MR, et al. Antisense oligodeoxynucleotide inhibition of tumor necrosis factor-alpha expression is neuroprotective after intracerebral hemorrhage. Stroke 2001; 32: 240–8.

Minghetti L. Role of COX-2 in inflammatory and degenerative brain diseases. Subcell Biochem 2007; 42: 127–41.

Palladino MA, Bahjat FR, Theodorakis EA, Moldawer LL. Anti-TNF-alpha therapies: the next generation. Nat Rev Drug Discov 2003; 2: 736–46.

Pompl PN, Ho L, Bianchi M, McManus T, Qin W, Pasinetti GM. A therapeutic role for cyclooxygenase-2 inhibitors in a transgenic mouse model of amyotrophic lateral sclerosis. FASEB J 2003; 17: 725–7.

Prevot A, Mosig D, Martini S, Guignard JP. Nimesulide, a cyclooxygenase-2 preferential inhibitor, impairs renal function in the newborn rabbit. Pediatr Res 2004; 55: 254–60.

Sawyer T. Withdrawing support for withdrawing support from premature infants with severe intracranial hemorrhage. Pediatrics 2008; 121: 1071–2; author reply 1072–3.

Shennan AH, Bewley S. Why should preterm births be rising? BMJ 2006; 332: 924–5.

Stephens BE, Vohr BR. Neurodevelopmental outcome of the premature infant. Pediatr Clin North Am 2009; 56: 631–46; table of contents.

Tobinick EL, Gross H. Rapid improvement in verbal fluency and aphasia following perispinal etanercept in Alzheimer's disease. BMC Neurol 2008; 8: 27.

Zhang X, Luhrs KJ, Ryff KA, Malik WT, Driscoll MJ, Culver B. Suppression of nuclear factor kappa B ameliorates astrogliosis but not amyloid burden in APPswe/PS1dE9 mice. Neuroscience 2009; 161: 53–8.

Zia MT, Csiszar A, Labinskyy N, Hu F, Vinukonda G, Lagamma EF, et al. Oxidative-nitrosative stress in a rabbit pup model of germinal matrix hemorrhage. Role of NAD(P)H oxidase. Stroke 2009; 40: 2191–8.